ORGANOMETALLICS

ARTICLE

pubs.acs.org/Organometallics

# N-Heterocyclic Carbene-Amide Rhodium(I) Complexes: Structures, Dynamics, and Catalysis

Luigi Busetto,[†] M. Cristina Cassani,*[,†] Cristina Femoni,[†] Michele Mancinelli,[‡] Andrea Mazzanti,[‡] Rita Mazzoni,*[,†] and Gavino Solinas[†]

[†]Dipartimento di Chimica Fisica ed Inorganica, Università degli Studi di Bologna, Viale Risorgimento 4, I-40136 Bologna, Italy

[‡]Dipartimento di Chimica Organica "A. Mangini", Università degli Studi di Bologna, Viale Risorgimento 4, I-40136 Bologna, Italy

Supporting Information

**ABSTRACT:** The amide-functionalized imidazolium salts $[BocNHCH_2CH_2ImR]X$ (R = Me, X = I, **1a**; R = benzyl, X = Br, **1b**; R = trityl, X = Cl, **1c**) bearing increasingly bulky N-alkyl substituents were prepared in high yields by direct alkylation of the (2-imidazol-1-yl-ethyl)carbamic acid *tert*-butyl ester; **1c** is a crystalline solid also characterized by X-ray diffraction. These salts are precursors for the synthesis of rhodium(I) complexes $[Rh(NBD)X(NHC)]$ (NHC = 1-(2-NHBoc-ethyl)-3-R-imidazolin-2-ylidene; X = Cl, R = Me (**3a**), R = benzyl (**3b**), R = trityl (**3c**); X = I, R = Me (**4a**)). All the complexes display restricted rotation about the metal−carbene bond; however, while the rotation barriers calculated for **3a**,**b** and **4a** matched the experimental values, unexpectedly this was not true in the case of **3c**, where the experimental value was equal to that obtained for compound **3b** (58.6 kJ $mol^{-1}$) and much smaller with respect to the calculated one (100.0 kJ $mol^{-1}$). The catalytic activity of the neutral rhodium(I) complexes **3a**−**c** in the hydrosilylation of terminal alkynes with $HSiMe_2Ph$ has been investigated with PhC≡CH, TolC≡CH, $^nBuC{\equiv}CH$, $Et_3SiC{\equiv}CH$, and $(CPh_2OH)C{\equiv}CH$ as substrates. The steric hindrance on the N-heterocyclic ligand and on the alkyne substrates affects conversion and selectivity: for the former the best results were achieved employing the less encumbered **3a** catalyst with TolC≡CH, whereas by employing hindered alkynes such as $Et_3SiC{\equiv}CH$ or $(CPh_2OH)C{\equiv}CH$ the hydrosilylation leads only to the formation of the $\beta$-(*E*)-vinylsilane and $\alpha$-bis(silyl)alkene isomers. The complexes **3a**,**b** have also been employed in the addition of arylaldehydes with phenylboronic acid, and like in the hydrosylylation case, the best results were obtained using **3a** in the presence of aldehydes bearing electron-withdrawing groups, such as 4-cyanobenzaldehyde and 4-acetylbenzaldehyde as substrates.

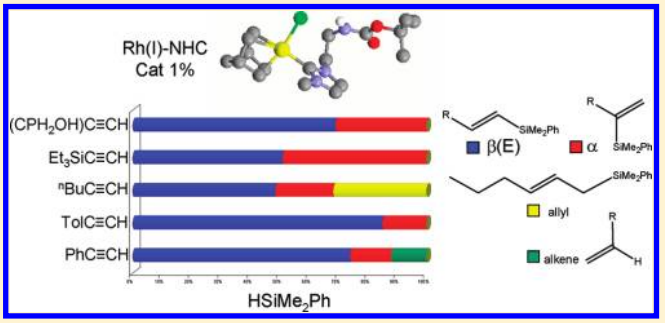


## 1. INTRODUCTION

N-Heterocyclic carbenes (NHCs) have attracted considerable attention as a new class of ligands over the past decade.[1] The heterocyclic carbene moiety offers great possibilities for fine-tuning the ligand structure and, thereby, the catalytic properties, through the introduction of appropriate substituents at the nitrogen atoms or at the five-membered-ring carbon atoms. The use of heteroatom-functionalized NHC carbenes in which a donor group is attached to a strongly bonded imidazolyl ring in the design of homogeneous catalysts has received increasing attention, as it can provide coordination versatility and enhanced catalytic activity.[2] In this context, amino/amide-functionalized NHC ligands are found to be important building blocks of active transition metal catalysts that are used for cross-coupling and hydrosilylation reactions.[3] With regard to the latter class of reaction, most of the recent efforts concern the design of efficient catalysts for the hydrosilylation of alkynes aimed at the selective formation of (*Z*) and (*E*)-alkenylsilanes.[4] Surprisingly the role played in such reactions by rhodium(I) NHC complexes has been little investigated,[1b] and good yields and fair to good selectivities were reported by Oro[3d] when using rhodium(I) complexes with alkylamino-functionalized NHC ligands for the hydrosilylation of terminal alkynes. The addition of aryl boronic derivatives to carbonyl compounds represents another active field of research for [(NHC)Rh] catalysts:[1b] Furstner first, followed by Buchmeiser, demonstrated that "common" dialkyl- or diaryl-NHC rhodium complexes are efficient at +80 °C with 1 mol % catalyst loading for different substituted benzaldehyde, while Özdemir and co-workers have synthesized and tested a large number of different NHC architecture scaffolds,[5] including amino-functionalized benzimidazolylidene systems.[6]

In this research field we recently described the selective, high-purity synthesis of *tert*-butyloxylcarbonyl (Boc)-protected 1-(2-aminoethyl)-3-methylimidazolium $[R^1NHCH_2CH_2ImR]X$ (**1a**, Im = imidazole, $R^1$ = Boc, R = Me, X = I, Chart 1) and deprotected $[NH_2CH_2CH_2ImMe]^+$. We had found that when the amino group is protected, the formation of stable silver

**Received:** July 13, 2011
**Published:** September 09, 2011

  

Chart 1

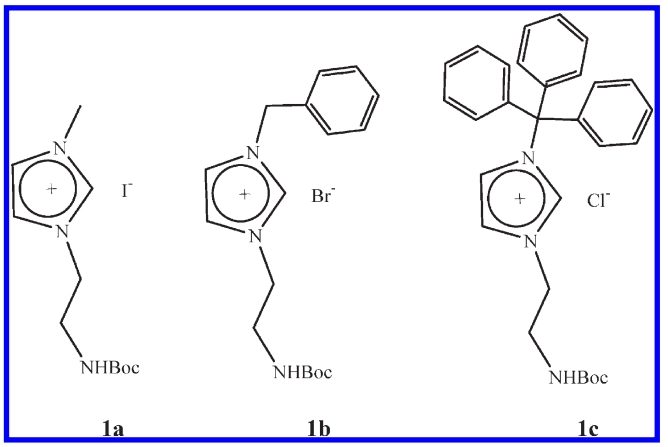


complexes with different bonding motifs in the solid state occurred, while with the deprotected ligand a silver complex of the type $[(NHC\text{-}NH_2)AgI]$ is likely to form, but it is unstable in solution.[7] The studies relative to the coordinating properties of the Boc-protected amino-functionalized imidazolium cation $[NH(Boc)CH_2CH_2ImMe]^+$ also revealed that the presence of the Boc group significantly reduces the nucleophilic power of the nitrogen atom on the side arm that never coordinates to the metal center. Successively $[NH_2CH_2CH_2ImMe]^+$ has been employed in the preparation of a gold(III)-aminoethyl imidazolium aurate salt, $[Cl_3AuNH_2(CH_2)_2ImMe)][AuCl_4]$,[8] used as a well-defined ionic liquid-stabilized $Au_{NPs}$ precursor.[9,10]

Following our initial report,[7] in this work we describe the synthesis and characterization of novel functionalized NHC ligand precursors of the type $[NH(Boc)CH_2CH_2ImR]^+$ (**1b**, R = benzyl; **1c**, R = trityl) and their silver(I) and rhodium(I) complexes. The dynamic behavior of the rhodium systems has been investigated by means of VT NMR studies and DFT calculations, and the application of these complexes in the hydrosilylation of alkynes as well as the addition of arylaldehydes to phenylboronic acid is also described.

## RESULTS AND DISCUSSION

**Synthesis of Imidazolium Ligand Precursors and NHC-Silver Complexes.** The novel imidazolium salts $[BocNHCH_2CH_2ImR]X$ (**1b**, R = benzyl, X = Br; **1c**, R = trityl, X = Cl) bearing increasingly bulky N-alkyl substituents were prepared in high yields by alkylation of the (2-imidazol-1-yl-ethyl)carbamic acid *tert*-butyl ester respectively with benzyl bromide and trityl chloride in dichloromethane at room temperature (Chart 1).

Like **1a**, the salt **1b** was isolated as a colorless to pale yellow viscous liquid, whereas **1c** is a crystalline solid; they are soluble in chlorinated solvents and were fully characterized by elemental analysis, NMR spectroscopy, electrospray ionization mass spectrometry (ESI-MS), and in case of **1c** also X-ray diffraction. The NMR resonances of the imidazolium fragment were observed at chemical shifts typical for imidazolium salts, and it is worth noting that, to the best of our knowledge, substitution at the 1,3-positions of the imidazole unit with the trityl group has been reported only in one case regarding rhodium-catalyzed hydrosilylation/cyclization reactions.[11]

Crystals of **1c** suitable for single-crystal X-ray diffraction were grown from a double layer of dichloromethane and petroleum ether (1:4). The molecular structure is shown in Figure 1; crystal data and experimental details are presented in Table 2, while for the full list of bond lengths and angles see the Supporting Information. The single crystals selected for X-ray analysis crystallize in the centrosymmetric $P2_1/c$ space group ($Z = 4$), and the unit cell also contains four water molecules. The bond distances and angles are in the expected range compared to those of known imidazolium salts,[12] and also the N(1)−C(19) distance for the N−C(trityl) bond of 1.5016(16) Å is in keeping with literature data.[13] In the latter group two phenyl rings (C(7)−C(12) and C(13)−C(18)) are linked in a helical shape, whereas the third phenyl (C(1)−C(6)) generates a second helical system with imidazole.[14] The NH group is not involved in hydrogen bonds with the carbenic hydrogen, but, on the contrary, it acts as donor with one of the chloride counteranions (N(3)···Cl(1) = 3.262 Å). Each of the four water molecules (see Figure S1 in the Supporting Information) also has hydrogen bonds with two chloride anions (3.182 and 3.233 Å) and with the carbenic hydrogen (3.034 Å).

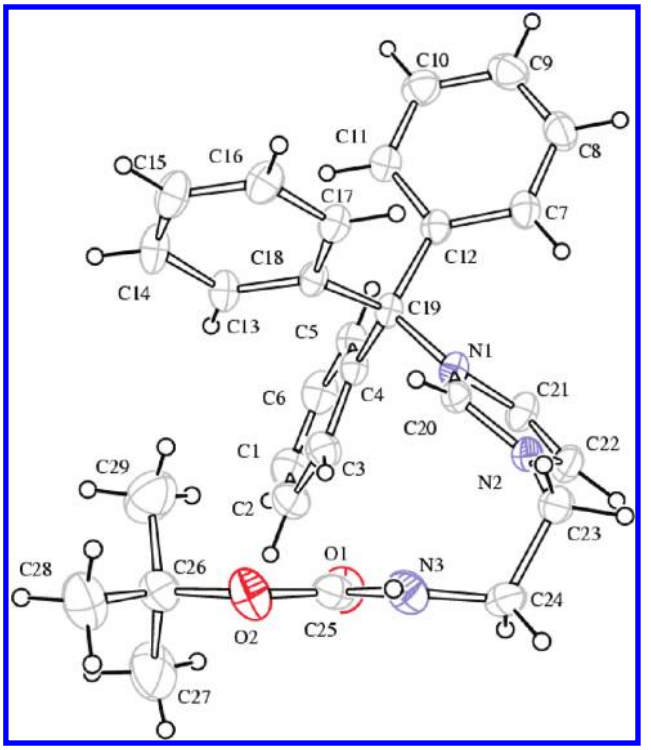


**Figure 1.** ORTEP diagram of **1c** depicted with displacement ellipsoids at the 30% probability level. The counterion and water molecules have been omitted for clarity.

Silver(I) halide complexes of NHC have been shown to be useful as NHC ligand transfer agents to metals,[15] and we have previously described that upon treatment of **1a** with $Ag_2O$ in a 2:1 stoichiometric ratio in dichloromethane, the biscarbene salt $[(NHC)_2Ag][AgI_2]$ (NHC = 1-(2-NHBoc-ethyl)-3-R-imidazolin-2-ylidene, R = Me, (**2a**)) is readily obtained.[7] Likewise, **1b** and **1c** have been successively reacted with $Ag_2O$ to give the silver complexes **2b,c**, although in the latter case longer reaction times (48 h instead of 2 h) are required due to the steric hindrance of the trityl group. The formation of **2b,c** was unambiguously confirmed by NMR spectroscopy and electrospray ionization mass spectrometry (ESI-MS); however, unlike what was previously done for **2a**,[7] the silver complexes were not


dx.doi.org/10.1021/om200631w |*Organometallics* 2011, 30, 5258–5272

**Scheme 1. Synthesis of Rhodium(I) Complexes**[a]

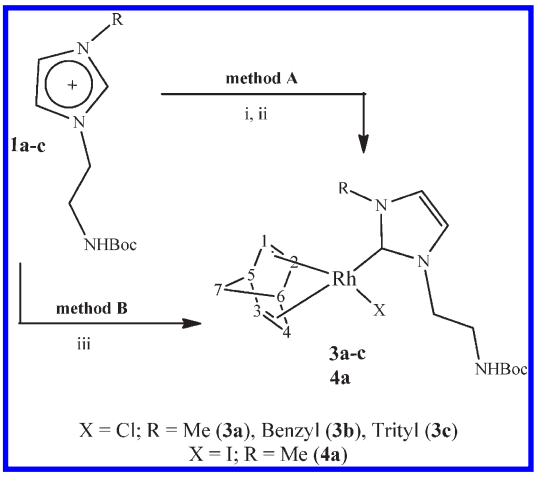


[a] Reactions and conditions for **3a**−**c**: (i) $Ag_2O$, $CH_2Cl_2$, RT; (ii) $[Rh(NBD)Cl]_2$, $CH_2Cl_2$, RT, 2 h. Reaction and conditions for **4a**: (iii) $[Rh(NBD)(O^tBu)]_2$, THF, RT, 3 h.

isolated but straightforwardly used *in situ*. The silver complexes **2b**,**c** showed $^1H$ and $^{13}C$ NMR in $CDCl_3$ features very similar to those previously described for **2a**: disappearance of the imidazolium NC*H*N proton resonance coupled with appearance of a singlet at ca. 180 ppm for the Ag−$C_{carbene}$ carbons. The electrospray ionization mass spectrometry analysis in methanol indicated the presence in solution of the cations $[(NHC)_2Ag]^+$ with the observed isotopic distributions in perfect agreement with the calculated ones.

**Synthesis of Rhodium(I) Complexes and Solution NMR Studies.** The rhodium complexes [Rh(NBD)Cl(NHC)] (NBD = 2,5-norbornadiene; **3a**, R = Me; **3b**, R = benzyl; **3c**, R = trityl) were synthesized by transmetalation from the NHC-Ag complexes **2a**−**c** in dichloromethane (Scheme 1, method A). The iodide analogue [Rh(NBD)I(NHC)] (**4a**, R = Me) was instead prepared either by reaction with the *in situ* generated carbene in THF (method B, reaction conditions iii) or by ion exchange methatesis from **3a** with an excess of NaI.[15]

We found that whereas the transmetalation reaction with $[Rh(NBD)Cl]_2$ always gave the yellow neutral mononuclear metal carbene complexes **3** in a very efficient and selective way (70−90% yield), with the synthetic procedure B the iodide complex **4a** was always isolated in lower yields (30−40%). This is probably due to the erratic oxidation of tetrahydrofuran to γ-butyrolactone catalyzed by Rh(I) (either the starting $[Rh(NBD)Cl]_2$ or the metal carbene itself) in the presence of trace amounts of water.[16] With the transmetalation method A, after filtering off any unreacted $Ag_2O$ or any formed AgX followed by gradient column chromatography under argon on anhydrous silica gel, complexes **3** were isolated as yellow microcrystalline solids. They are completely soluble in chlorinated solvents and acetonitrile, partially soluble in diethyl ether, and completely insoluble in petroleum ether. Complexes **3a**,**b** and **4a** are air sensitive in the solid state and in solution but not moisture sensitive: continuous monitoring of the NMR samples in $CDCl_3$ showed that decomposition to unidentified products rapidly occurs after exposure to air (ca. 1 h) but not after controlled additions of degassed water at either room temperature (over two weeks) or 55 °C (30 min.). On the contrary **3c** is perfectly air stable, and NMR monitoring for over 10 days of a sample prepared in air with not anhydrous chloroform did not present any significant decomposition.

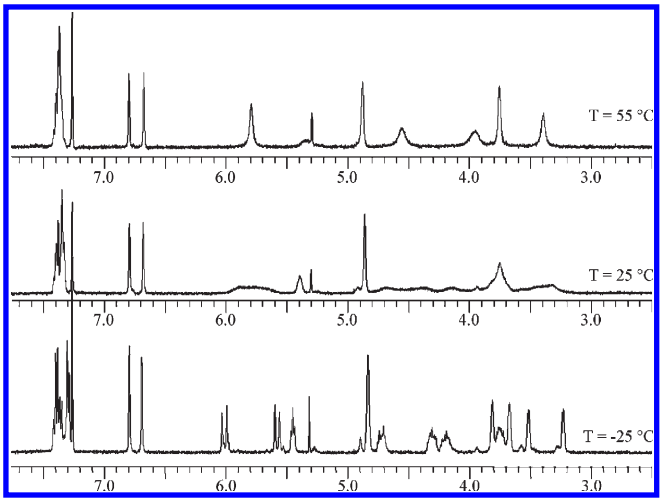


**Figure 2.** $^1H$ NMR of **3b** at various temperatures (600 MHz in $CDCl_3$).

They have been fully characterized by elemental analysis, ESI-MS mass spectrometry, and $^1H$ and $^{13}C$ NMR using gCOSY, gHSQC, and gHMBC experiments for full resonance assignments.

The $^1H$ NMR ($CDCl_3$) spectra for **3a** show a broad signal at 6.74 ppm assigned to the =CH backbone protons, while in the $^{13}C\{^1H\}$ NMR spectra the coordination of the carbene to the rhodium center becomes evident as a doublet resonance at 184.2 ppm (d, $J_{C,Rh}$ = 57.1 Hz). These chemical shifts and coupling constant values lie in the usual range for related Rh(I)-NHC complexes.[3d,17] The olefinic protons of the norbornadiene ligand feature three 1:1:1 resonances (2 protons each) at 4.86, 3.82, and 3.49 ppm, respectively, and three doublets in the $^{13}C\{^1H\}$ NMR spectra at 63.6 ($J_{C,Rh}$ = 4.8 Hz), 51.0 ($J_{C,Rh}$ = 4.8 Hz), and 48.1 ($J_{C,Rh}$ = 12.3 Hz). This observation can be explained by the lack of an effective symmetry plane in the molecules as the result of the hindered rotation about the carbene−rhodium bond. Due to the steric hindrance exerted by the two side arms, the norbornadiene moiety and the chlorine atom are displaced in an out-of-plane disposition with respect to the imidazole ring. If the two side arms are different, the molecule has $C_1$ symmetry; therefore a pair of conformational enantiomers is generated.

The $^1H$ spectra of compound **3b**, bearing a benzyl group, are displayed in Figure 2. The spectrum recorded at room temperature (middle trace) shows very broad signals, and, in particular, the signal of the benzylic $CH_2$ is close to the coalescence point. When the temperature is raised to +55 °C, all the signals sharpen, whereas on lowering the temperature, the benzylic $CH_2$ decoalesces into an AB system (5.58 and 6.02 ppm) and the methylenic protons of the amide side arm splits into diastereotopic signals too. The carbonyl stretching frequency (νCO) of the carbamic group −NHC(O)O− does not give any information on the kind of coordination and is similar to that of the starting imidazolium precursor always appearing at about 1710 $cm^{-1}$ for the rhodium complexes, and although the complexes are neutral, positive ESI-MS analyses for the complexes **3a**−**c** and **4a** always showed a major $m/z$ peak corresponding to the $[M - X]^+$ fragment.

All attempts to facilitate a κN coordination of the amine nitrogen by removing the halide ligand as AgX resulted in decomposition products even when the reactions were performed in

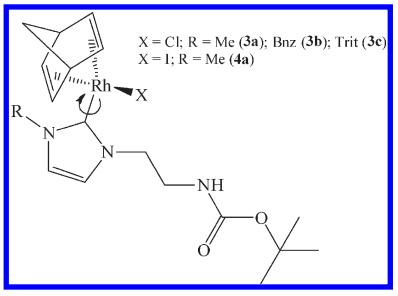


Figure 3

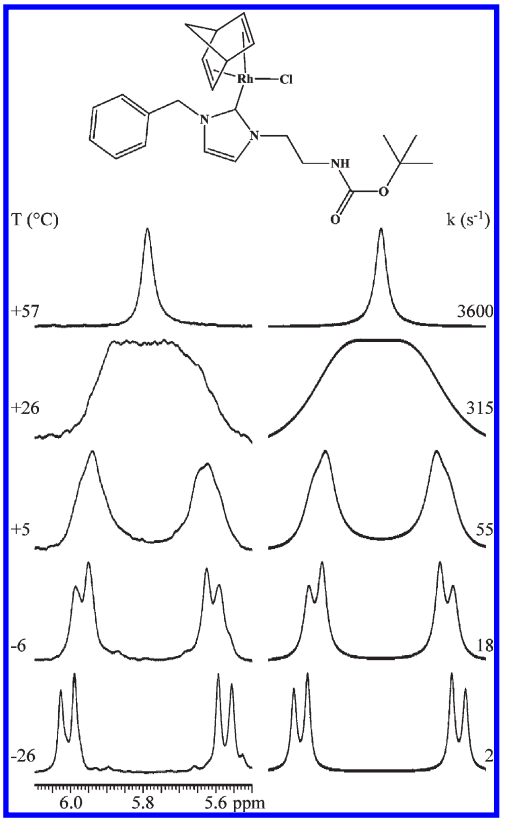


**Figure 4.** Variable-temperature spectra of **3b** showing the evolution of the benzylic $CH_2$ signal ($^1$H NMR at 400 MHz in $CDCl_3$). On the right the simulations with the corresponding rate constants are reported.

coordinating solvents (acetone or acetonitrile) and/or in the presence of coordinating anions (triflate).

**Stereodynamics.** The stereodynamics and the rotation barriers about the Rh—carbene bond have been determined by making use of variable-temperature NMR spectroscopy,[19] on increasing the steric hindrance of the N-alkyl substituent, and by varying the halogen atom (Figure 3).

In the case of **3b**, the signal of the benzylic $CH_2$ shows the typical shape of the coalescence at +25 °C. As shown in Figure 4, the signal sharpens at high temperature, whereas it decoalesces into an AB system at low temperature. Line shape simulation at various temperatures yielded the rate constants for the enantiomerization, from which an activation energy of 58.6 kJ mol$^{-1}$ was derived by the Eyring equation. The activation energy was found to be constant with respect to the temperature, indicating a negligible value of the activation entropy. This implies that the

**Scheme 2. (Left) Experimental X-ray Structures of 3a and 4a; (Right) Calculated Structures**

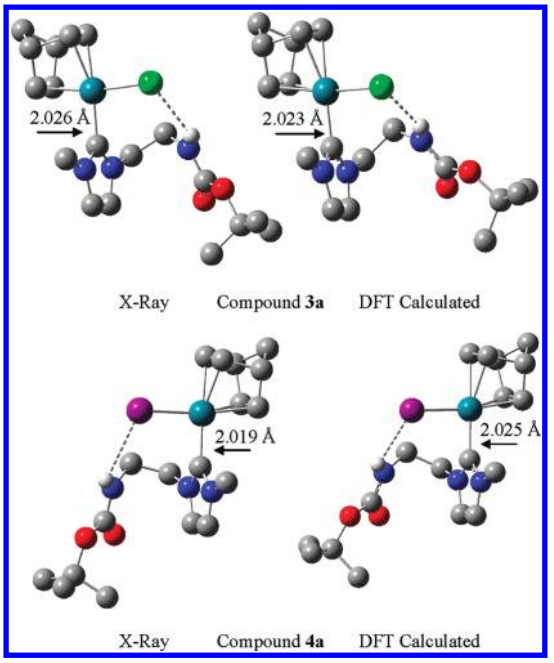


observed barrier should be due to steric effects only. When the steric hindrance on one side arm is reduced, as in compound **3a**, the rotational barrier is lower (55.3 kJ mol$^{-1}$), and the enantiomerization process could be monitored by observing the splitting of a CH signal of norbornadiene (Figure S6). On the contrary, when the chlorine atom of **3a** is exchanged with iodine (as in compound **4a**), the rotational barrier is increased, and the signals of norbornadiene are split at room temperature. On raising the temperature, the coalescence point is reached at +57 °C, and a single broad signal was observed at +90 °C (spectra at higher temperatures cannot be recorded due to decomposition). The rotational barrier was derived to be 72.4 kJ mol$^{-1}$ (Figure S7). These data agree very well with those of Enders and Gielen, confirming a steric origin of the rotation barrier.[20]

An analogous behavior is observed for **3c** (Figures S2—S5); moreover the presence of the three phenyl rings of the trityl group causes a ring current effect that leads to a significant downfield shift of one of the $NCH_2$— wingtip diasterotopic protons that is found at 6.02 ppm, whereas on the opposite, a proton of the norbornadiene is high-field shifted to an unusually low 2.1 ppm.

The variable-temperature spectra taken in the case of compound **3c** (Figure S8) showed that the rotational barrier (58.8 kJ mol$^{-1}$) was identical, within error, to that obtained in the case of the benzyl-substituted compound **3b**; however, the spectra simulations show a noticeable increase of the free energy of activation on raising the temperature, therefore indicating a negative entropic activation.

DFT calculations of compounds **3a**—**c** and **4a** were performed at the B3LYP/LANL2DZ level. The geometry of the calculated ground states of **3a** and **4a** were almost identical to that observed in the solid state (Scheme 2). In particular the calculations correctly reproduced the Rh—C, Rh—Cl, and Rh—I bond lengths. In addition, the torsion angles that generate the two conformational enantiomers observed in solution were also correctly reproduced (Cl(2)—Rh(1)—C(8)—N(2) = 89.15°;


dx.doi.org/10.1021/om200631w |*Organometallics* 2011, 30, 5258–5272

**Scheme 3. Enantiomerization Pathway for Compounds 3a−c and 4a**

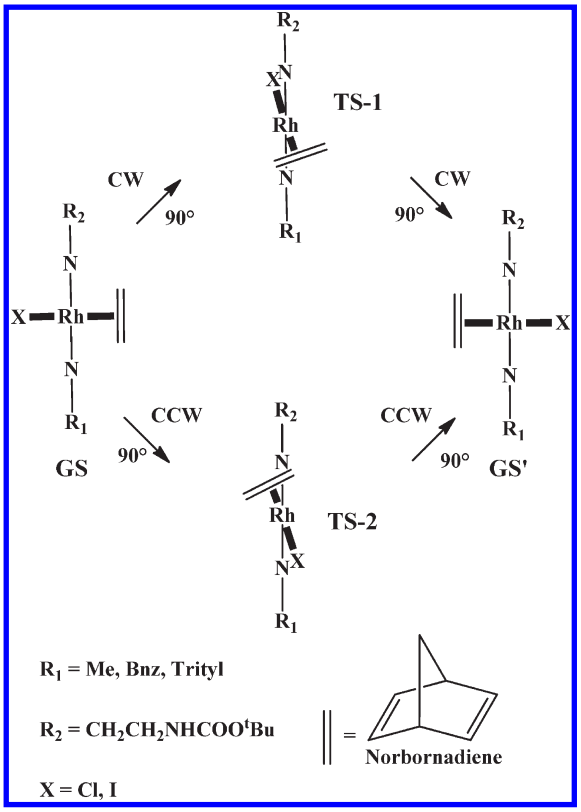


**Table 1. Calculated and Experimental Energy Barriers for the Enantiomerization of 3a−c and 4a (energies in kJ mol$^{-1}$, calculations at the B3LYP/LANL2DZ level)**

| compd | TS-1 | TS-2 | exptl (kJ mol$^{-1}$) |
|---|---|---|---|
| **3a** | 58.8 | 67.8 | 55.3[a] |
| **3b** | 67.9 | 77.7 | 58.6[a] |
| **3c** | 100.0 | 126.4 | 58.8[b] |
| **4a** | 79.2 | 83.3 | 72.4[a] |

[a] $\Delta G^{\ddagger}$ invariant with the temperature. [b] $\Delta G^{\ddagger}$ at −1.5 °C. $\Delta H^{\ddagger}$ = 46.1 kJ mol$^{-1}$; $\Delta S^{\ddagger}$ = −43 J K$^{-1}$ mol$^{-1}$.

I(1)−Rh(1)−C(8)−N(9) = 96.72°). These results actually show that the theoretical level employed in the calculations is suitable to tackle the conformational analysis of these complexes.

The two enantiomeric ground states GS and GS′ can interconvert into each other by two possible transition states due to the rotation around the carbene−rhodium bond (Scheme 3). The first one (TS-1) is reached by a 90° clockwise rotation starting from GS and corresponds to the crossing of the halogen atom on the $CH_2$ of the amide-ethyl moiety (denoted as $R_2$), whereas the second transition state (TS-2) takes place when a counterclockwise rotation forces the halogen to cross the second alkyl side arm group ($R_1$) on the imidazole. The steric hindrance of the halogen and $R_1$ obviously influence the activation energy of the rotational barrier. DFT calculations of the two possible transition states (see Table 1) suggested that the threshold pathway (i.e., that with the lowest transition-state energy) corresponded in all the cases to the passage of the halogen atom on the amide-ethyl group (TS-1), with the simultaneous crossing of the norbornadiene on the second side arm (R1). The calculations also suggested that the energy barrier is strongly related to the steric hindrance of $R_1$, and for this reason the barrier calculated for compound **3c** is predicted to be very high (100.0 kJ mol$^{-1}$).

While the rotation barriers calculated for **3a** and **3b** matched the experimental values, this was not true in the case of **3c**, where the experimental value was equal to that obtained for compound **3b** and much smaller with respect to the calculated one. In addition, the energy barrier derived for **3c** from line shape simulation showed a strong dependence on the temperature, while the barriers measured for **3a,b** did not show this effect. In particular, the large negative activation entropy derived from simulations (−40 ± 10 eu) indicates that a strongly organized transition state or a different interconversion pathway could take place in the case of compound **3c**. The inversion process may proceed either via a cleavage of the Rh−Cl bond before or during the rotation[21] or by partial dissociation of the trityl group into a contact ionic pair, followed by the rotation of the Rh−Cl moiety and subsequent re-formation of nitrogen−trityl carbon bond.[22] The experimental evidence that the replacement of chlorine with iodine raises the rotational barrier in the case of **3a** and **4a** (as correctly indicated also by the calculations) suggests that the latter hypothesis should be considered more likely. In addition, the possible coordination of a phenyl ring of the trityl moiety to rhodium[23] in the transition state might be responsible for the partial dissociation of the trityl group and for lowering the energy of the transition state. In this framework the value obtained for compound **3c** is a threshold value for the true steric rotational barrier.

**Crystal Structure Determination for 3a, 4a, and 3c.** The molecular structures of the rhodium(I) complexes **3a**, **4a**, and **3c** were determined via X-ray diffraction and are reported in Figures 5, 6, and 7, respectively. The crystal data and experimental details together with the Rh−$C_{carbene}$ and R−X distances are reported in Table 2, whereas the full list of bond lengths and angles are reported in the Supporting Information. The structural analysis confirmed that the Boc protection removes most of the nucleophilicity of the amide nitrogen that is never involved in any coordinative bond. Crystals of **3a** and **4a** suitable for diffraction were grown by slow evaporation of a mixture of $CH_2Cl_2$ and petroleum ether.

The structure of **3a**, which crystallized in a centric space group ($P2_1/c$), consists of separated $C_{18}H_{27}ClN_3O_2Rh$ molecules arranged in eclipsed, alternating columns of enantiomers. There are, in fact, two possible orientations of the $BocNHCH_2CH_2$− and $-CH_3$ substituents on the functionalized imidazolium ring, and both are generated by the cell symmetry operators from the unique Rh complex in the asymmetric unit. Rhodium shows a classic square-planar coordination and is bonded to the Cl(2) atom, the carbenic C(8) atom, and the bidentate norbornadiene fragment. The stronger trans effect that the carbene exercises compared with the chlorine ligand is inferable from the distances between Rh and C atoms on the norbornadiene unit: the Rh−C(1) and Rh−C(2) contacts trans to the carbene are 2.204(2) and 2.206(2) Å, respectively, and the Rh−C(3) and Rh−C(4) bond lengths trans to Cl atom are remarkably shorter, both 2.083(2) Å. Despite the presence of donor chlorides anions, there are not significant intra- or intermolecular hydrogen bonds in the solid state, with the exception of a very weak intermolecular interaction between Cl(2) and N(3) (3.366 Å). In addition

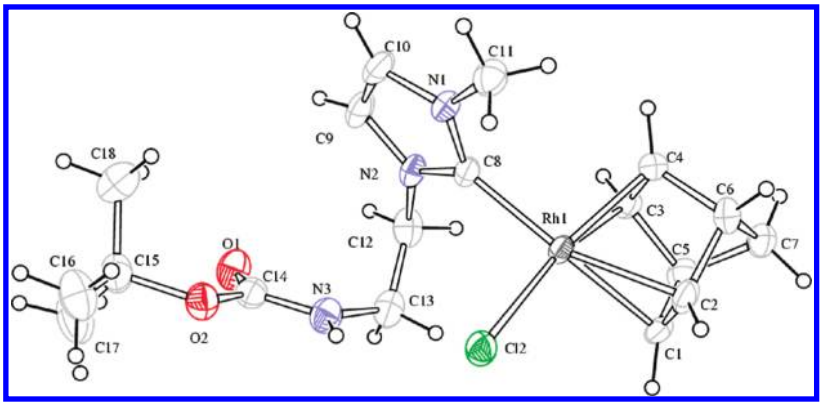


**Figure 5.** ORTEP diagram of **3a** depicted with displacement ellipsoids at the 30% probability level.

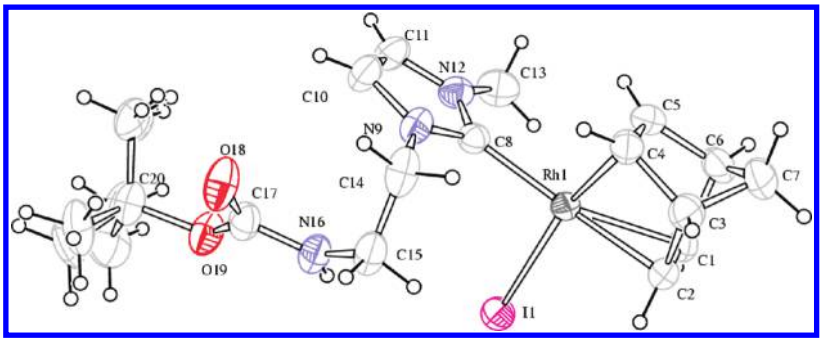


**Figure 6.** ORTEP diagram of **4a** depicted with displacement ellipsoids at the 30% probability level.

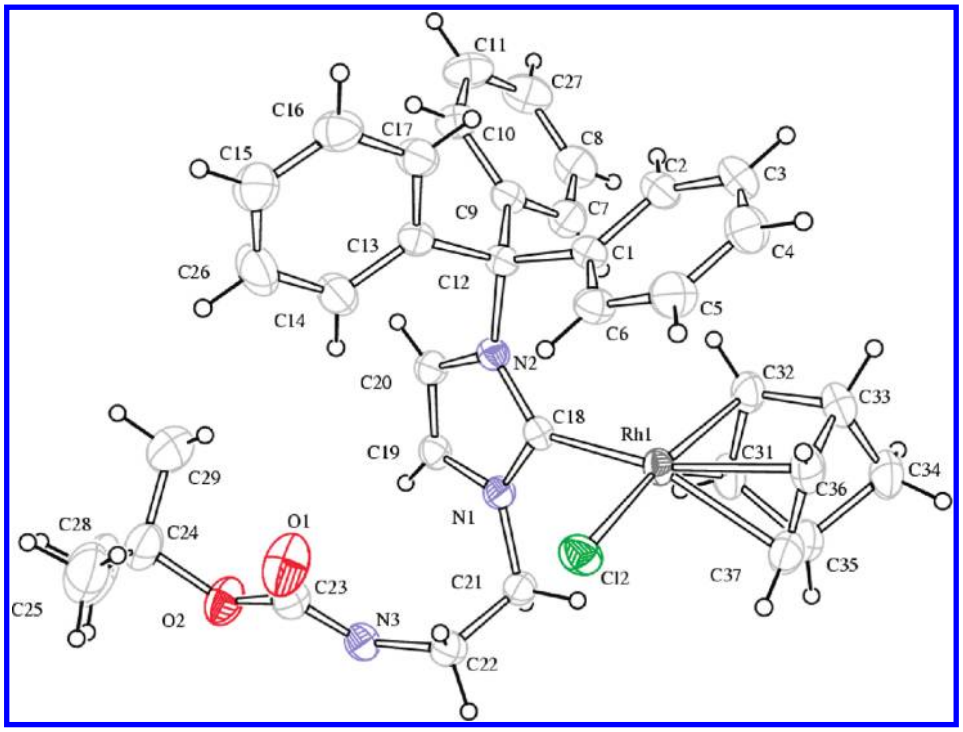


**Figure 7.** ORTEP diagram of **3c** depicted with displacement ellipsoids at the 30% probability level.

there is no evidence of a positional disorder in the structure even at room temperature, and this is an index of the very high efficient solid packing of the molecules, which is mainly stabilized by steric effects.


dx.doi.org/10.1021/om200631w |*Organometallics* 2011, 30, 5258–5272

Table 2. Crystal Data and Data Collection and Refinement Parameters for 1c, 3a, 4a, and 3c

| | 1c·$H_2O$ | 3a | 4a | 3c·$2CH_3CN$ |
|---|---|---|---|---|
| formula | $C_{29}H_{34}ClN_3O_3$ | $C_{18}H_{27}ClN_3O_2Rh$ | $C_{18}H_{27}IN_3O_2Rh$ | $C_{40}H_{45}ClN_5O_2Rh$ |
| fw | 508.04 | 455.79 | 547.24 | 766.17 |
| $T$, K | 296(2) | 298(2) | 296(2) | 296(2) |
| $\lambda$, Å | 0.71073 | 0.71073 | 0.71073 | 0.71073 |
| cryst syst | monoclinic | monoclinic | monoclinic | monoclinic |
| space group | $P2_1/c$ | $P2_1/c$ | $P2_1/c$ | $P2_1/n$ |
| $a$, Å | 8.5286(9) | 11.9725(7) | 12.0829(13) | 13.1294(13) |
| $b$, Å | 17.2903(18) | 18.1627(10) | 15.0838(16) | 9.7921(10) |
| $c$, Å | 18.910(2) | 9.9190(5) | 12.2761(13) | 29.874(3) |
| $\alpha$, deg | 90 | 90 | 90 | 90 |
| $\beta$, deg | 93.2710(10) | 112.3730(10) | 108.2450(10) | 93.5440(10) |
| $\gamma$, deg | 90 | 90 | 90 | 90 |
| cell volume, $Å^3$ | 2751.8(5) | 1994.55(19) | 2124.7(4) | 3833.4(7) |
| $Z$ | 4 | 4 | 4 | 4 |
| $D_c$, g $cm^{-3}$ | 1.226 | 1.518 | 1.711 | 1.328 |
| $\mu$, $mm^{-1}$ | 0.173 | 1.006 | 2.272 | 0.555 |
| $F(000)$ | 1080 | 936 | 1080 | 1592 |
| cryst size, mm | 0.80 × 0.70 × 0.60 | 0.30 × 0.25 × 0.20 | 0.20 × 0.15 × 0.10 | 0.60 × 0.40 × 0.20 |
| $\theta$ limits, deg | 1.61 to 28.71 | 1.84 to 25.00 | 1.77 to 25.00 | 1.37 to 28.72 |
| index ranges | $-10 \le h \le 11$, $-22 \le k \le 21$, $-24 \le l \le 25$ | $-14 \le h \le 14$, $-21 \le k \le 21$, $-11 \le l \le 11$ | $-14 \le h \le 14$, $-17 \le k \le 17$, $-14 \le l \le 14$ | $-17 \le h \le 17$, $-13 \le k \le 13$, $-40 \le l \le 39$ |
| reflns collected | 31 214 | 18 769 | 20 041 | 43 389 |
| indep reflns | 6711 [$R$(int) = 0.0219] | 3513 [$R$(int) = 0.0209] | 3740 [$R$(int) = 0.0449] | 3740 [$R$(int) = 0.0276] |
| completeness to $\theta$ = 25.00° | 100.0% | 100.0% | 100.0% | 100.0% |
| data/restraints/params | 6711/0/348 | 3513/0/226 | 3740/24/255 | 9350/0/459 |
| goodness on fit on $F^2$ | 0.903 | 1.030 | 1.009 | 0.998 |
| $R_1$ ($I > 2\sigma(I)$) | 0.0419 | 0.0217 | 0.0303 and 0.0623 | 0.0319 |
| $wR_2$ (all data) | 0.1139 | 0.0617 | 0.0503 and 0.0717 | 0.0759 |
| largest diff peak and hole, e $Å^{-3}$ | 0.235 and −0.289 | 0.388 and −0.283 | 0.639 and −0.634 | 0.519 and −0.277 |
| Rh−C bond length (Å) | | 2.026(2) | 2.020(4) | 2.0549(18) |
| Rh−X bond length (Å) | | 2.3794(6) | 2.6597(5) | 2.4283(6) |

The structure of **4a** (Figure 6), which crystallized in the same centric space group as its chloride congener, does not significantly differ from the latter in terms of solid-state packing and atomic coordination, the only exception being a slight positional disorder found in the terminal *tert*-butyl group of the ligand. Again the complex crystallized in a racemic mixture with both enantiomers present in a 1:1 ratio. The same strong trans effect of the carbenic atom C(8) is also observed, as revealed by the Rh−C bond lengths: the Rh−C(1) and Rh−C(2) distances, in trans position with respect to C(8), are both 2.207(4) Å, while the Rh−C(4) and Rh−C(5) bonds, trans to the I atom, are 2.103(4) and 2.105(4) Å in that order.

Crystals of **3c** suitable for X-ray diffraction were obtained from a concentrated acetonitrile solution at −20 °C.

Compound **3c** crystallizes in the centrosymmetric $P2_1/n$ group, and both enantiomers are generated by the center of symmetry, as in the previous cases. At variance with **3a** and **4a**, the unit cell contains also eight molecules of acetonitrile, which makes the crystal package less efficient. As in the case of **3a** and **4a**, the rhodium has a square-planar coordination, with the Rh−Cl and Rh−$C_{carbene}$ bond distances slightly longer with respect to **3a** (2.055 Å for Rh(1)−C(18) and 2.428 Å for Rh(1)−Cl(2); see Table 2). This could be ascribed to the steric hindrance exerted by the large trityl group. The dihedral angle Cl(2)−Rh(1)−C(18)−N(2) that yields the two enantiomers whose barrier was observed in solution is 111°, to be compared with that of 92.47° observed for Cl(2)−Rh(1)−C(8)−N(1) in **3a**.

**Catalysis.** The potential of the Rh(I) complexes **3a**−**c** as catalysts as well as the influence of the carbene substituents on the catalytic activity was examined in the hydrosilylation of 1-alkynes and in the addition of aryladehydes to phenylboronic acid.

*Hydrosilylation of 1-Alkynes.* The complexes were found to be active catalyst precursors for the hydrosilylation of terminal alkynes. The catalytic reactions were carried out in $CDCl_3$ at +25 °C using a slight excess of $HSiMe_2Ph$ and were routinely monitored by $^1H$ NMR spectroscopy. The influence of the 1-alkyne has been studied using phenylacetylene, tolylacetylene, 1-hexyne, (triethylsilyl)acetylene, and 1,1-diphenyl-2-propyn-1-ol as substrates (Table 3).[24] Catalyst loadings as low as 0.5 and 0.1 mol % of **3a** also provided high activities at room temperature (Table 3, entries 12−15), although in the latter case slower kinetics were found.

As generally reported for transition metal catalyzed hydrosilylation of 1-alkynes,[4b] and in particular for neutral and cationic Rh(I)-NHC hydrosilylation catalysts,[3d] the reaction is unselective, and complexes **3a**−**c** convert phenylacetylene and tolylacetylene to a


dx.doi.org/10.1021/om200631w |*Organometallics* 2011, 30, 5258–5272

mixture of the three possible isomeric vinylsilane derivatives: $\beta$-(*Z*)- or $\beta$-(*E*)-1-silyl-1-alkenes from the anti-Markovnikov addition and $\alpha$-2-silyl-1-alkene from the Markovnikov addition. Furthermore the formation of the corresponding alkene has been observed from these substrates (Scheme 4, Figure 8).[25]

Although **3a**−**c** completely converted all the substrates, the less encumbered **3a** showed the best reaction rates; for instance in the phenylacetylene case turnover frequencies (TOF) of 48 $h^{-1}$ were found for **3a**, 40 $h^{-1}$ for **3b**, and 13 $h^{-1}$ for **3c** (see also the profile of conversion of PhC≡CH with **3a**−**c** in Figure 9; further details on substrate profiles of conversion and selectivity vs time are available in the Supporting Information, Figures S9−S21).

Contrary to what was reported by Oro et al. employing similar amino-alkyl-functionalized rhodium complexes,[3d] in the hydrosilylation of phenylacetylene we did not observe the formation of polyphenylacetylene. The $\beta$-(*Z*) vinylsilane is the major product until the substrate completely disappears. However, once complete conversion is reached, $\beta$-(*Z*) isomerizes to $\beta$-(*E*) vinylsilane, which, at the end of the reaction, is always the major product (bar diagram in Figure 8). In Figure 10 we report an example of conversion and selectivity profiles vs time for the reaction of PhC≡CH and dimethylphenylsilane catalyzed by **3a**. The graph shows that $\beta$-(*Z*) and $\beta$-(*E*) vinylsilane profiles cross when the conversion is complete, and the reaction goes further until $\beta$-(*Z*) completely converts to $\beta$-(*E*). We can also observe that the formation of an $\alpha$ isomer (10−12%) and styrene (14−16%) (alkene in Scheme 4 and Figures 8 and 10) affects the selectivity of the reaction.

Data for the other catalysts and substrates reported in Table 3 and Figures 11 and 12 (see the Supporting Information for further graphs and details) show that the $\alpha$ isomer is always identified in variable amounts, 11−49%, while the alkene formation only affected the phenyl and tolylacetylene substrates (Figures 8 and 11). The best results in terms of selectivity have been obtained employing **3a** as catalyst and tolylacetylene as the substrate: this reaction leads to the formation of $\beta$-(*E*) (85%) and $\alpha$ isomers (15%) within 6 h, whereas no alkene formation has been observed in this case.

When $^n$BuC≡CH is employed as substrate (Table 3, Figure 12), the reaction rate is generally slower, showing with **3a** a TOF of 24 $h^{-1}$ (cf. with phenylacetylene TOF = 48 $h^{-1}$ and tolylacetylene TOF = 50 $h^{-1}$). Furthermore once the conversion is complete, the $\beta$-(*Z*) vinylsilane isomerizes into the hex-2-enyldimethylphenylsilane (allyl in Figure 12) (32−46%) instead of the $\beta$-(*E*) vinylsilane (Scheme 5). This behavior is in line with what was previously reported by Crabtree et al. in the hydrosilylation of 1-hexyne with $HSiMePh_2$ catalyzed by $[Rh(PPh_3)_3Cl]$.[25d]

It is worth noting that, as above stated, the hydrosilylation of 1-hexyne requires a longer initiation time (cf. Figure S10 with Figure 9 for phenylacetylene and Figure S9 for tolylacetylene). In view of the fact that the alkyne's steric encumbrance negatively affects the reaction rate (*vide infra*) and by comparison with literature data on the hydrosilylation of 1-hexyne,[3d,26] this behavior has to be ascribed to an electronic effect. In particular a less activated metal−alkyne bond could inhibit the catalyst turnover, slowing the insertion step.[27]

Opposite of what was observed with the previously discussed substrates (phenyl, tolyl, and *n*-butylacetylene) and in agreement with what was previously reported,[3d] the reaction of dimethylphenylsilane with (triethylsilyl)acetylene, $Et_3SiC{\equiv}CH$, in the presence of **3a** leads to the formation of only the two isomers $\beta$-(*E*) and $\alpha$. This behavior has been attributed to both the steric hindrance and the electronic characteristics of the precursor and can be confirmed catalyzing the reaction between 1,1-diphenyl-2-propyn-1-ol, $(CPh_2OH)C{\equiv}CH$, and dimethylphenylsilane with **3a**: also in this case only the formation of the $\beta$-(*E*) and $\alpha$ isomers occurred, with a better selectivity in the former (Figure 11, Scheme 6).

**Table 3. Hydrosilylation of Terminal Alkynes**

| entry | alkyne | cat.[a] | conv (% NMR) | % $\beta$-(*E*) | % $\beta$-(*Z*) | % $\alpha$ | % alkene |
|---|---|---|---|---|---|---|---|
| 1 | PhC≡CH | **3a** | 95 | 21 | 63 | 16 | |
| 2 | PhC≡CH | **3b** | 79 | 24 | 50 | 15 | 11 |
| 3 | PhC≡CH | **3c** | 26 | 32 | 19 | 21 | 28 |
| 4 | TolC≡CH | **3a** | >99 | 54 | 33 | 13 | |
| 5 | TolC≡CH | **3b** | 76 | 27 | 48 | 13 | 12 |
| 6 | TolC≡CH | **3c** | 26 | 43 | 27 | 31 | |
| 7 | $^n$BuC≡CH | **3a** | 48 | 33 | 40 | 27 | |
| 8 | $^n$BuC≡CH | **3b** | 32 | 42 | 58 | | |
| 9 | $^n$BuC≡CH | **3c**[b] | 0 | 0 | 0 | 0 | |
| 10 | $Et_3SiC{\equiv}CH$ | **3a** | >99 | 51 | | 49 | |
| 11 | $(CPh_2OH)C{\equiv}CH$ | **3a** | 47 | 67 | | 33 | |
| 12 | PhC≡CH | **3a**[c] | 94 | 24 | 55 | 16 | 5 |
| 13 | TolC≡CH | **3a**[c] | >99 | 46 | 36 | 13 | 3 |
| 14 | PhC≡CH | **3a**[d] | 72 | 31 | 26 | 22 | 20 |
| 15 | TolC≡CH | **3a**[d] | 68 | 30 | 48 | 18 | 4 |

[a] Reaction time = 2 h; catalyst loading (1 mol %) unless otherwise stated. [b] In this case the substrate conversion presented a longer induction time: after 24 h the conversion achieved 26% (selectivities: % $\beta$-(*E*) = 37%; % $\beta$-(*Z*) = 42%; % $\alpha$ = 21%). [c] Catalyst loading (0.5 mol %). [d] Catalyst loading (0.1 mol %).

**Scheme 4**

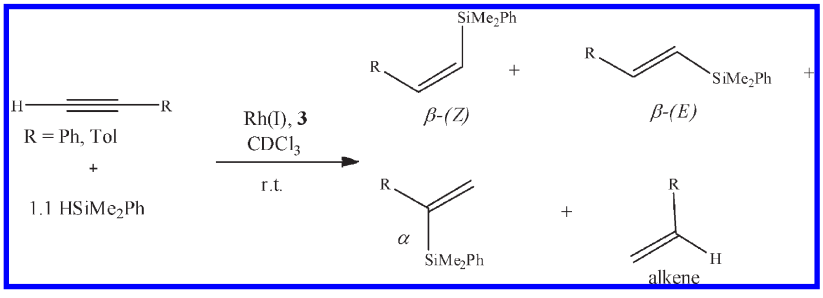



dx.doi.org/10.1021/om200631w |*Organometallics* 2011, 30, 5258–5272

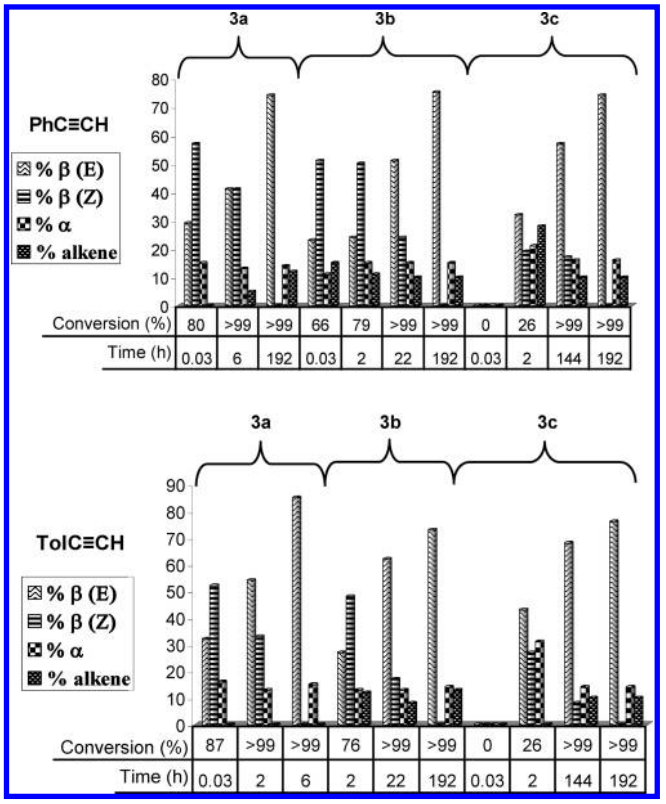


**Figure 8.** Selectivity vs conversion and time for the hydrosilylation of phenylacetylene (top) and tolylacetylene (bottom) catalyzed by **3a**, **3b**, and **3c**.

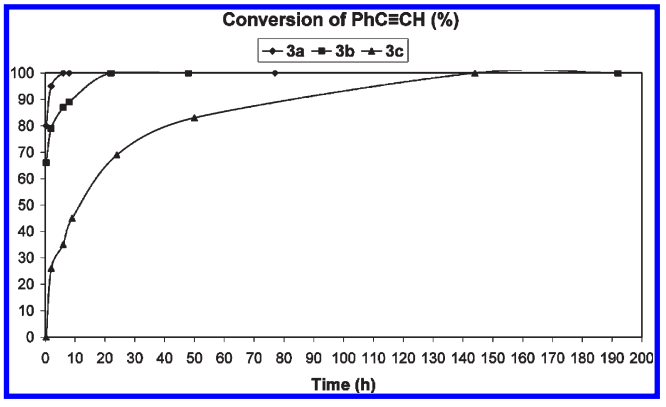


**Figure 9.** Reaction profile of conversion vs time for the hydrosilylation of PhC≡CH with complexes **3a**, **3b**, and **3c**.

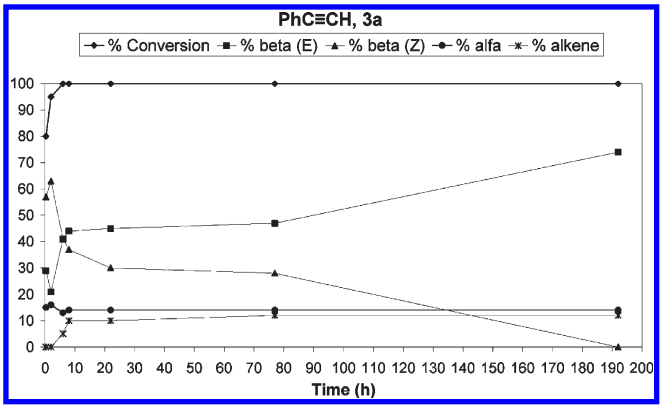


**Figure 10.** Reaction profile of conversion and selectivities vs time for the hydrosilylation of PhC≡CH with **3a**.

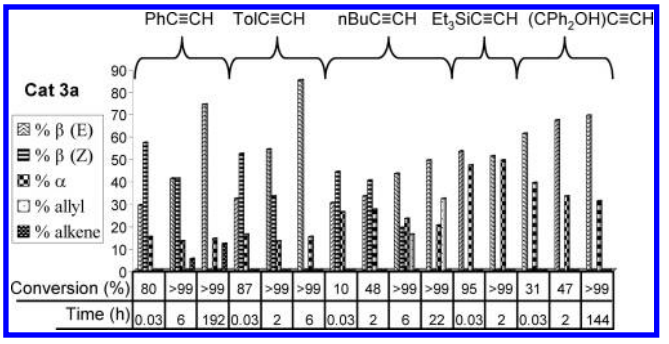


**Figure 11.** Selectivity vs conversion and time for the hydrosilylation of all the substrates under study catalyzed by **3a**.

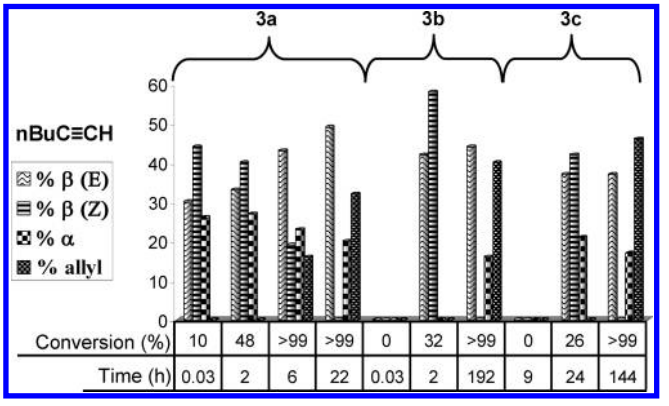


**Figure 12.** Selectivity vs conversion and time for the hydrosilylation of butylacetylene catalyzed by **3a**, **3b**, and **3c**.

By comparing the alkyne conversions when employing the less encumbered catalyst **3a**, we can observe that the steric encumbrance of the alkyne also affects the reaction rate. While all the other substrates completely convert within 6 h, the tertiary propargyl alcohol $(CPh_2OH)C{\equiv}CH$ reaches complete conversion only after 144 h (Figure 11).

Generally while the reaction rate is affected by the steric encumbrance of both the complexes **3a**−**c** and the alkynes, the substituents on the N-heterocyclic ring of the catalysts **3a**−**c** do not seriously affect the selectivity, which is otherwise influenced by the steric hindrance and electronics of the alkyne. This behavior is in accordance with the mechanism proposed for neutral and cationic amino rhodium NHC complexes.[3d]

*Addition of Arylaldehydes to Phenylboronic Acid.* The complexes **3a** and **3b** were also found to be active catalyst precursors for the addition of aryladehydes to phenylboronic acid.[28] The catalytic reactions were carried out in dimethoxyethane/water (3:1) in the presence of the aldehyde, an equimolar amount of $KO^tBu$, and an excess of phenylboronic acid, heating at +80 °C in the presence of rhodium carbene catalyst (1% mol) (Scheme 7).


dx.doi.org/10.1021/om200631w |*Organometallics* 2011, 30, 5258–5272

Scheme 5

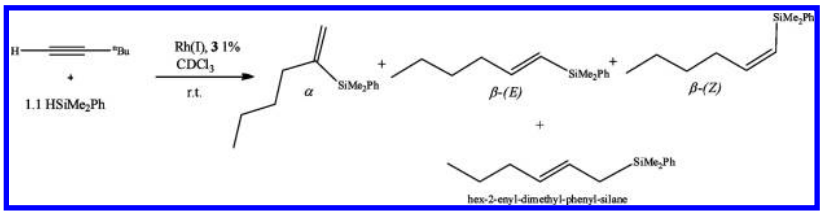


Scheme 6

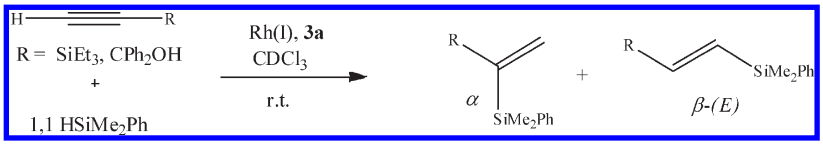


Scheme 7

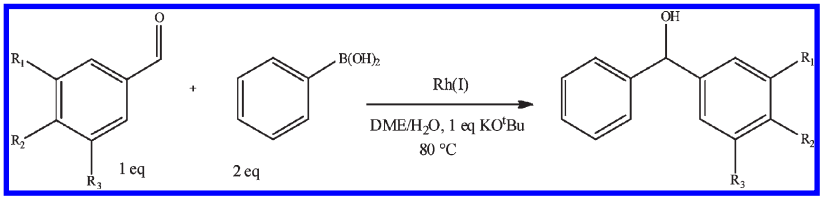


**Table 4. Addition of Arylaldehydes with Phenylboronic Acid**

| entry | aldehyde | catalyst | time (h) | conv (%) | yield (%) |
|---|---|---|---|---|---|
| 1 | 4-Cl-PhCHO | **3a** | 5 | 99 | 78 |
| 2 | 4-Cl-PhCHO | **3b** | 5 | 83 | 80 |
| 3 | 4-OMe-PhCHO | **3a** | 8 | 42 | 38 |
| 4 | 4-OMe-PhCHO | **3b** | 8 | 32 | 29 |
| 5 | 3,4,5-(tri-OMe)-PhCHO | **3a** | 8 | 66 | 63 |
| 6 | 3,4,5-(tri-OMe)-PhCHO | **3b** | 8 | 45 | 42 |
| 7 | 4-$^t$Bu-PhCHO | **3a** | 8 | 66 | 43 |
| 8 | 4-$^t$Bu-PhCHO | **3b** | 8 | 49 | 39 |
| 9 | 4-CN-PhCHO | **3a** | 1 | 99 | 87 |
| 10 | 4-CN-PhCHO | **3b** | 1 | 96 | 75 |
| 11 | 4-C(O)Me-PhCHO | **3a** | 2 | 99 | 82 |
| 12 | 4-C(O)Me-PhCHO | **3b** | 2 | 99 | 80 |

Conversions and isolated yields were monitored by $^1$H NMR spectroscopy.[29] The influence of the aldehyde has been studied using 4-chlorobenzaldehyde, 4-methoxybenzaldehyde, 3,4,5-trimethoxybenzaldehyde, 4-*tert*-butylbenzaldehyde, 4-cianobenzaldehyde, and 4-acetylbenzaldehyde. The results are summarized in Table 4.

Catalysts **3a**,**b** convert all the tested aldehydes in moderate to good yields. Better results have been obtained by employing the less encumbered **3a** catalyst, which was shown to be faster in all cases (e.g., TOFs for **3a** and **3b** with 4-Cl-PhCHO as substrate are 20 and 16 h$^{-1}$, respectively), and employing electron-withdrawing −CN- and −C(O)Me-functionalized aldehydes (e.g., with 4-CN-PhCHO the TOF for **3a** is 99 h$^{-1}$), which quantitatively convert (NMR) within 2 h with high isolated yields (entries 9−12). When lowering the electron deficiency of the aldehydes, the conversions and reaction rates contextually decrease (entries 1−8). This behavior is in line with what was reported by Miyaura for rhodium-catalyzed addition of arylboronic acid to aldehydes, giving secondary alcohols, which is in general facilitated by the presence of an electron-withdrawing group on the aldehydes,[30] and with the results obtained by Imlinger and Buchmeiser for rhodium 1,3-R$_2$-tetrahydropyrimidin-2-ylidenes, indicating the need for a highly nucleophilic metal center.[5d]

## CONCLUSIONS

We have described the synthesis of novel imidazolium salts that are precursors for rhodium(I) complexes [Rh(NBD)X(NHC)] (NHC = 1-(2-NHBoc-ethyl)-3-R-imidazolin-2-ylidene; X = Cl, R = Me (**3a**), R = benzyl (**3b**), R = trityl (**3c**); X = I, R = Me (**4a**)), in which the NHC ligands bear an amide functional group on one nitrogen and increasing bulky N-alkyl substituents (Me, benzyl, trityl) on the other. All the complexes display restricted rotation about the metal−carbene bond; however while the rotation barriers calculated for the complexes in which R = Me, benzyl (**3a**,**b** and **4a**) matched the experimental values, this was not true in the trityl case **3c**, where the experimental value was equal to that obtained for compound **3b** and much smaller with respect to the calculated one. In addition, the energy barrier derived for **3c** from line shape simulation showed a strong dependence on the temperature, while the barriers measured for **3a**,**b** did not show this effect. In particular, the large negative activation entropy derived from simulations (−40 ± 10 eu) indicates that a strongly organized


dx.doi.org/10.1021/om200631w |*Organometallics* 2011, 30, 5258–5272

transition state and a different interconversion pathway takes place in the case of compound **3c**. We believe that these observations may bring important implications in further research in NHC−M formation, and studies in this direction are in progress.

The neutral rhodium(I) complexes **3a**−**c** are efficient catalyst precursors for the hydrosilylation of terminal alkynes. The steric hindrance on the N-heterocyclic ligand and on the alkyne substrates affects conversion and selectivity: for the former the best results have been obtained employing the less encumbered **3a** catalyst with tolylacetylene and dimethylphenylsilane as substrates, whereas by employing hindered alkynes such as $Et_3SiC{\equiv}CH$ or $(CPh_2OH)C{\equiv}CH$ the hydrosilylation leads only to the formation of $\beta$-(*E*) and $\alpha$ isomers. The complexes **3a**,**b** have also been employed in the addition of arylaldehydes with phenylboronic acid, and like in the hydrosilylation case, the best results were obtained using **3a** in the presence of aldehydes bearing electron-withdrawing groups, such as 4-cyanobenzaldehyde and 4-acetylbenzaldehyde as substrates. Studies concerning the use of the deprotected imidazolium salt $[NH_2CH_2CH_2ImMe]^+$ as precursor for a primary-amino-functionalized NHC ligand are under way.

## EXPERIMENTAL SECTION

**Materials and Procedures.** All reactions were carried out under argon using standard Schlenk techniques. Solvents were dried and distilled under nitrogen prior to use; the deuterated solvents used after being appropriately dried and degassed were stored in ampules under argon on 4 Å molecular sieves. The prepared derivatives were characterized by elemental analysis and spectroscopic methods. The IR spectra were recorded with a FT-IR Perkin-Elmer Spectrum 2000 spectrometer. The NMR spectra were recorded using Varian Inova 300 ($^1$H, 300.1; $^{13}$C, 75.5 MHz), Varian MercuryPlus VX 400 ($^1$H, 399.9; $^{13}$C, 100.6 MHz), Varian Inova 600 ($^1$H, 599.7; $^{13}$C, 150.8 MHz) instruments. The spectra were referenced internally to residual solvent resonances, and unless otherwise stated, they were recorded at 298 K for characterization purposes; full $^1$H and $^{13}$C NMR assignments were done, when necessary, by gCOSY, gHSQC, gHMBC, and NOESY NMR experiments using standard Varian pulse sequences; J.Young valve NMR tubes (Wilmad) were used to carry out NMR experiments under inert conditions. ESI-MS analyses were performed by direct injection of methanol solutions of the metal complexes using a Waters ZQ 4000 mass spectrometer. Elemental analyses were performed on a ThermoQuest Flash 1112 Series EA instrument. The chemicals 2-bromoethylamine hydrobromide, imidazole (ImH), benzyl bromide, and $Ag_2O$ were used as purchased from Aldrich; $[Rh(NBD)Cl]_2$ was purchased from Strem and used as received; the starting building blocks—2-*t*-Boc-aminoethyl bromide (carbamic acid 2-bromoethyl-*tert*-butyl ester),[31] (2-imidazol-1-yl-ethyl)carbamic acid *tert*-butyl ester ($BocNHCH_2CH_2Im$),[7,32] 1-(2-BocNH-ethyl-)-3-methylimidazolium iodide (**1a**), 1-(2-BocNH-ethyl)-3-methylimidazolin-2-ylidenesilver iodide (**2a**)[7]—were prepared according to literature procedures. Phenylacetylene, 1-hexyne, 4-ethynyltoluene, triethylsilylacetylene, 1,1-diphenyl-2-propyn-1-ol, dimethyphenylsilane, 4-chlorobenzaldehyde, 4-methoxybenzaldehyde, 3,4,5-trimethoxybenzaldehyde, 4-*tert*-butylbenzaldehyde, 4-cianobenzaldehyde, 4-acetylbenzaldehyde, and phenylboronic acid were used as purchased from Sigma Aldrich. Petroleum ether (Etp) refers to a fraction of bp 60−80 °C. The reactions were monitored by thin-layer chromatography (TLC) on highly purified silica gel on polyester (w/UV indicator) and visualized using UV light (254 nm). Column chromatography was carried out under argon on silica gel previously heated at about 200 °C while a slow stream of a dry nitrogen was passed through it;[33] Celite was dried in an oven at 150 °C. Melting points were taken with a Stuart Scientific SMP3 melting point apparatus and were uncorrected.

*Synthesis of Triphenylchloromethane (Trityl Chloride).* This product was synthesized using a modified literature method.[34] A three-neck, dry, round-bottom flask was charged with triphenylmethanol (4.0 g, 15.4 mmol) and dry toluene (10 mL) under argon. A condenser was attached, and the mixture was heated to 80 °C. Acetyl chloride (1.1 mL, 15.4 mmol) was added with a dropping funnel while stirring vigorously with a magnetic stirrer. Once the solid had dissolved, additional acetyl chloride (1.90 mL, 27.8 mmol) was added over the course of 10 min. The solution was heated for 30 min and then cooled in an ice bath, and petroleum ether (80 mL) was added. This mixture was left in the ice bath for 2 h, at which point a dark brown product separated out and was discarded. Volatiles were removed from the filtrate under vacuum to give a pale yellow solid, which after washing with petroleum ether (3 × 5 mL) and drying afforded the title compound as an off-white powder (3.34 g, 78%) that must be stored under argon. $^1$H NMR (300.1 MHz, $CDCl_3$): $\delta$ 7.34−7.25 (m, Ph). $^{13}C\{^1H\}$ NMR (75.50 MHz, $CDCl_3$): $\delta$ 145.25 ($C_5$), 129.67 ($C_4$), 127.76 ($C_2$), 127.71 ($C_3$), 81.34 ($C_1$).

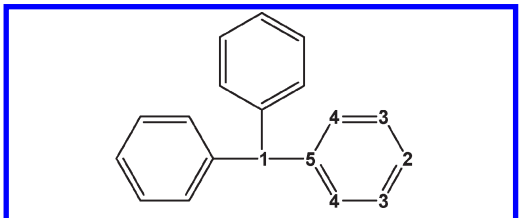

Trityl and phenyl group numbering scheme

*Synthesis of 1-(2-BocNH-ethyl-)-3-benzylimidazolium Bromide,* ***1b***. In a 100 mL round-bottom flask to a solution of $BocNHCH_2CH_2Im$ (1.02 g, 4.80 mmol) in $CH_2Cl_2$ (10 mL) was added an excess of benzyl bromide (7.20 mmol). After stirring for 12 h at room temperature, the solvent was removed under vacuum, and the resulting pale yellow, viscous oil was thoroughly washed with diethyl ether (3 × 10 mL). After separation from the washings the oil was kept under vacuum at 40 °C for several hours to yield 1.87 g (100%) of **1b**. $^1$H NMR (399.9 MHz, $CDCl_3$): $\delta$ 10.20 (s, 1H, NC*H*N), 7.45 (s, 1H, $CH_{im}$), 7.35−7.27 (m, 5H, Ph), 7.22 (s, 1H, $CH_{im}$), 6.12 (br s, 1H, NH), 5.52 (s, 2H, $PhCH_2N$), 4.56 (br t, 2H, $NCH_2$), 3.69 (br t, 2H, $CH_2NH$), 1.36 (s, 9H, $CH_3$). $^{13}C\{^1H\}$ NMR (100.6 MHz, $CDCl_3$): $\delta$ 156.1 (C═O), 137.9 (CH, NCHN), 132.7 (Ph, $C_5$), 128.9 (Ph, $2C_4$), 128.8 (Ph, $2C_3$), 128.3 (Ph, $C_2$), 123.3 ($CH_{im}$), 121.4 ($CH_{im}$), 79.4 (Cq, $^t$Bu), 53.3 ($PhCH_2$), 49.5 ($NCH_2$), 40.2 ($CH_2NH$), 28.6 ($CH_3$, $^t$Bu). IR ($CH_2Cl_2$, $cm^{-1}$): 1706 (vs, $\nu_{CO}$); (neat, $cm^{-1}$): 3399 (vs, $\nu_{NH}$), 3136, 3068, 2977, 1701 (vs, $\nu_{CO}$), 1560, 1509, 1457, 1366, 1255, 1164. ESI-MS (MeOH, *m*/*z*): 302 (100) $[M]^+$; 79 (97), 81 (100) $[Br]^-$. Anal. Calcd (%) for $C_{17}H_{24}BrN_3O_2$: C, 53.41; H, 6.33; N, 10.99. Found: C, 53.80; H, 6.62; N, 11.33.

*Synthesis of 1-(2-BocNH-ethyl-)-3-tritylimidazolium Chloride,* ***1c***. In a 100 mL round-bottom flask to a solution of $BocNHCH_2CH_2Im$ (0.93 g, 4.41 mmol) dissolved in $CH_2Cl_2$ (20 mL) was added trityl chloride (1.30 g, 4.66 mmol). After stirring for 16 h at room temperature, the solvent was removed under vacuum and the resulting solid was thoroughly washed with diethyl ether (3 × 10 mL) to yield 2.05 g (95%) of a white solid identified as **1c**. $^1$H NMR (399.9 MHz, $CDCl_3$): $\delta$ 9.12 (s, 1H, NC*H*N), 8.01 (s, 1H, $CH_{im}$), 7.39 (m, 9H, Ph), 7.13 (m, 6H, Ph), 6.96 (s, 1H, $CH_{im}$), 6.61 (br s, 1H, NH), 4.78 (t, 2H, $J_{H,H}$ = 5.5 Hz, $NCH_2$), 3.61 (m, 2H, $J_{H,H}$ = 5.4 Hz, $CH_2NH$), 1.31 (s, 9H, $CH_3$). $^{13}C\{^1H\}$ NMR (100.6 MHz, $CDCl_3$): $\delta$ 156.6 (C═O), 139.5 ($C_5$), 137.3 (NCHN), 129.5 ($C_4$), 129.3 ($C_2$), 128.9 ($C_3$), 123.5 ($CH_{im}$), 123.3 ($CH_{im}$), 79.5 (Cq, $^t$Bu), 79.2 (C1), 49.9 ($NCH_2$), 40.5 ($CH_2NH$), 28.3 ($CH_3$, $^t$Bu). IR ($CH_2Cl_2$, $cm^{-1}$): 1707 (vs, $\nu_{CO}$); (KBr, $cm^{-1}$):

3368 (vs, $\nu_{NH}$), 3166, 3144, 3061, 2977, 1702 (vs, $\nu_{CO}$), 1493, 1446, 1365, 1252, 1168. ESI-MS (MeOH, *m/z*): 454 (100) $[M]^+$. Anal. Calcd (%) for $C_{29}H_{32}ClN_3O_2$: C, 71.09; H, 6.58; N, 8.58. Found: C, 71.16; H, 6.50; N, 8.65. Mp = 68 °C. Crystals of **1c** suitable for single-crystal X-ray diffraction were grown from a double layer of dichloromethane and petroleum ether (1:4) at room temperature.

*Preparation of [Rh(NBD)Cl{1-(2-NHBoc-ethyl)-3-R-imidazolin-2-ylidene}], R = Me (**3a**), Bnz (**3b**), Trit (**3c**).* **Synthesis of 3a.** To a solution of **1a** (0.258 g 0.73 mmol) in $CH_2Cl_2$ (ca. 30 mL) was added $Ag_2O$ (0.107 g, 0.37 mmol). The suspension was stirred for 2 h and filtered on Celite, and the filtrate was added to a solution of $[Rh(NBD)Cl]_2$ (0.168 g 0.37 mmol) in $CH_2Cl_2$. After stirring for 3 h the yellow AgI was filtered off, and the solvent was removed under vacuum. The crude material was purified by column chromatography on silica gel using first $CH_2Cl_2$ and then $CH_2Cl_2$/MeOH [100:3 (v/v)] as eluent to afford 0.23 g (71%) of **3a** as a yellow solid. $R_f$: 0.60 ($CH_2Cl_2$/MeOH, 100:5). $^1$H NMR (300.1 MHz, $CDCl_3$): $\delta$ 6.76 (br s, 2H, $CH_{im}$), 5.34 (br s, 1H, NH), 4.86 (m, 2H, NBD), 4.49 (m, 2H, $NCH_2$), 4.10 (s, 3H, $NCH_3$), 3.92 (m, 2H, $CH_2NH$), 3.82 (m, 2H, NBD), 3.49 (m, 2H, NBD), 1.41 (s, 9H, $^t$Bu), 1.36 (t, 2H, $J_{H,H}$ = 1.4 Hz, $C^7H_2$ NBD). $^{13}C\{^1H\}$ NMR (75 MHz, $CDCl_3$): $\delta$ 184.2 (d, $J_{C,Rh}$ = 57.1 Hz), 156.3 (C═O), 121.8 ($CH_{im}$), 121.6 ($CH_{im}$), 79.4 (d, $J_{C,Rh}$ = 4.6 Hz, NBD), 79.2 (Cq, $^t$Bu), 63.6 (d, $J_{C,Rh}$ = 4.8 Hz; NBD), 51.0 (d, $J_{C,Rh}$ = 2.4 Hz, NBD), 49.6 ($NCH_2$), 48.1 (d, $J_{C,Rh}$ = 12.3 Hz, NBD), 41.3 ($CH_2NH$), 37.9 ($NCH_3$), 28.4 ($CH_3$, $^t$Bu). IR ($CH_2Cl_2$, $cm^{-1}$): 1712 (vs, $\nu_{CO}$). IR (KBr, $cm^{-1}$): 3386 (s, $\nu_{NH}$), 3156, 3120, 3104, 3056, 3041, 2981, 2922, 1700 $cm^{-1}$ (vs, $\nu_{CO}$), 1500, 1364, 1254, 1173. ESI-MS (MeOH, *m/z*): 478 (11) $[M + Na]^+$, 420 (100) $[M - Cl]^+$; 490 (100) $[M + Cl]^-$. Anal. Calcd (%) for $C_{18}H_{27}ClN_3O_2Rh$: C, 47.43; H, 5.97; N, 9.22. Found: C, 47.10; H, 6.04; N, 9.23. Mp = 136 °C (dec). Suitable crystals of **3a** for X-ray diffraction have been obtained by slow evaporation from a mixture of $CH_2Cl_2$ and petroleum ether.

**Synthesis of 3b.** To a solution of **1b** (0.500 g, 1.31 mmol) in $CH_2Cl_2$ (30 mL) was added $Ag_2O$ (0.154 g, 0.66 mmol). After stirring for 2 h at room temperature, the suspension was filtered on Celite and the filtrate added to a solution of $[Rh(NBD)Cl]_2$ (0.301 g, 0.65 mmol) in $CH_2Cl_2$. After 3 h, AgBr was filtered off and the solvent was removed under vacuum. The crude material was purified by column chromatography on silica gel using first $CH_2Cl_2$ and then $CH_2Cl_2$/MeOH, 100:1 (v/v), as eluent to afford 0.67 g (78%) of **3b** as a yellow solid. $R_f$: 0.65 ($CH_2Cl_2$/MeOH, 100:5).

The silver intermediate of 1-(2-BocNH-ethyl)-3-benzylimidazolin-2-ylidene, silver bromide **2b**, was not isolated, but a NMR and ESI-MS analysis was carried out on the crude material to confirm its formation. $^1$H NMR of **2b** (399.9 MHz, $CDCl_3$): $\delta$ 7.21−6.98 (m, 5H, Ph), 7.02 (s, 1H, $CH_{im}$), 6.81 (s, 1H, $CH_{im}$), 5.74 (br s, $^1$H, NH), 5.14 (s, 2H, $PhCH_2N$), 4.16 (br t, 2H, $NCH_2$), 3.39 (br t, 2H, $CH_2NH$), 1.28 (s, 9H, $CH_3$). $^{13}C\{^1H\}$ NMR (100.6 MHz, $CDCl_3$): $\delta$ 181.5 (s, C-Ag), 155.9 (C═O), 135.7 (Ph, $C_5$); 128.7 (Ph, $C_4$); 128.1 (Ph, $C_3$); 127.3 (Ph, $C_2$), 122.0 ($CH_{im}$), 120.9 ($CH_{im}$), 78.9 (Cq, $^t$Bu), 55.2 ($CH_2$, $PhCH_2$), 51.1 ($CH_2$, $NCH_2$), 41.2 ($CH_2$, $CH_2NH$), 28.1 ($CH_3$, $^t$Bu). IR ($CH_2Cl_2$, $cm^{-1}$): 1707 (vs, $\nu_{CO}$). ESI-MS (MeOH, *m/z*): 709 (100) $[C_{34}H_{46}AgN_6O_4]^+$; 79 (100), 81 (97) $[Br]^-$.

$^1$H NMR of **3b** (599.7 MHz, $CDCl_3$, 228.18 K): $\delta$ 7.35 (m, 5H, Ph), 6.79 (d, 1H, $J_{H,H}$ = 1.8 Hz, $CH_{im}$), 6.68 (d, 1H, $J_{H,H}$ = 1.8 Hz, $CH_{im}$), 6.01 (d, 1H, $J_{H,H}$ = 15.2 Hz, $CH_2Ph$), 5.57 (d, 1H, $J_{H,H}$ = 15.2 Hz, $CH_2Ph$), 5.45 (t, 1H, $J_{H,H}$ = 5.6 Hz, NH), 4.83 (m, 2H, NBD), 4.70 (m, 1H, $NCH_2$); 4.31 (m, 1H, $NCH_2$), 4.18 (m, 1H, $CH_2NH$), 3.81 (m, 1H, NBD), 3.76 (m, 1H, $CH_2NH$), 3.67 (m, 1H, NBD), 3.51 (m, 1H, NBD), 3.23 (m, 1H, NBD), 1.39 (s, 9H, $CH_3$), 1.31 (d, 1H, $J_{H,H}$ = 8.1 Hz, $C^7H_2$, NBD), 1.26 (d, 1H, $J_{H,H}$ = 8.1 Hz, $C^7H_2$, NBD). $^{13}C\{^1H\}$ NMR (150.8 MHz, $CDCl_3$, 228.2 K): $\delta$ 185.2 (d, $J_{C,Rh}$ = 55.2), 156.3 (C═O), 136.8 (Ph, $C_5$); 128.9 (Ph, $C_4$); 128.6 (Ph, $C_3$); 128.1 (Ph, $C_2$), 122.3 ($CH_{Im}$), 120.5 ($CH_{Im}$), 79.3 (Cq, $^t$Bu), 79.2 (CH, NBD), 63.6 (d, $J_{C,Rh}$ = 4.8 Hz, $C^7H_2$, NBD), 54.5 ($CH_2$, $CH_2Ph$), 51.1 (d, $J_{C,Rh}$ = 15.7 Hz, CH, NBD), 49.4 (d, $J_{C-Rh}$ = 12.1 Hz, CH, NBD), 49.2 ($NCH_2$), 48.6 (d, $J_{C-Rh}$ = 11.5 Hz, CH, NBD), 41.8 ($CH_2NH$), 28.3 ($CH_3$, $^t$Bu). IR ($CH_2Cl_2$, $cm^{-1}$): 1710 (vs, $\nu_{CO}$). IR (KBr, $cm^{-1}$): 3340 (s, $\nu_{NH}$), 3167, 3123, 3091, 3060, 3032, 2978, 2928, 1708 $cm^{-1}$ (vs, $\nu_{CO}$), 1509, 1365, 1250, 1173. ESI-MS (MeOH, *m/z*): 554 (12) $[M + Na]^+$, 496 (100) $[M - Cl]^+$; 530 (100) $[M - H]^-$. Anal. Calcd (%) for $C_{24}H_{31}ClN_3O_2Rh$: C, 54.19; H, 5.87; N, 7.90. Found: C, 54.21; H, 5.89; N, 7.87. Mp = 97 °C.

**Synthesis of 3c.** To a solution of **1c** (0.200 g, 0.41 mmol) in $CH_2Cl_2$ (20 mL) was added $Ag_2O$ (0.050 g, 0.21 mmol). The suspension was stirred for 48 h, then solid $[Rh(NBD)Cl]_2$ (0.092 g, 0.20 mmol) was directly added to the reaction mixture. After stirring for a further 2 h the crude material was filtered on a Celite pad, the insoluble material was thoroughly washed with $CH_2Cl_2$, and the solvent was removed under vacuum. The residue was purified by column chromatography on silica gel treated with 5% v/v triethylamine in $Et_2O$, using $Et_2O/CH_2Cl_2$, 1:3 (v/v), to afford 0.22 g (78%) of **3c** as a yellow solid. $R_f$: 0.71 ($CH_2Cl_2$/MeOH, 100:5); $R_f$: 0.22 ($Et_2O$). Suitable crystals for an X-ray diffraction analysis were obtained from a concentrated solution of **3c** in $CH_3CN$ at −20 °C.

The silver intermediate **2c** was not isolated, but a $^1$H NMR and ESI-MS analysis was carried out on the crude material to confirm its formation. $^1$H NMR of **2c** (399.9 MHz, $CDCl_3$): $\delta$ 7.36−7.21 (m, 15H, Ph), 7.29 (s, 1H, $CH_{im}$), 7.03 (s, 1H, $CH_{im}$), 4.24 (t, 2H, $J_{H,H}$ = 6.0 Hz, $NCH_2$), 3.51 (t, 2H, $J_{H,H}$ = 6.0 Hz, $CH_2NH$), 1.43 (s, 9H, $^t$Bu), the NH resonance was not observed. $^{13}C\{^1H\}$ NMR (100.6 MHz, $CDCl_3$): $\delta$ 183.9 (s, C-Ag), 156.8 (C═O), 142.0 ($C_5$), 130.0 ($C_4$), 128.4 ($C_2$, $C_3$), 123.5 ($CH_{im}$), 119.5 ($CH_{im}$), 80.0 (C1), 79.9 (Cq, $^t$Bu), 52.6 ($NCH_2$), 41.4 ($CH_2NH$), 28.3 ($CH_3$, $^t$Bu). ESI-MS (MeOH, *m/z*): 1015 (50) $[C_{58}H_{64}AgN_6O_4]^+$, 243 (100) $[Ph_3C]^+$.

$^1$H NMR of **3c** (599.7 MHz, $CDCl_3$, 243.2 K): $\delta$ 7.38−7.17 (m, 15H, Ph), 6.98 (s, 1H, $CH_{im}$), 6.46 (s, 1H, $CH_{im}$), 6.02 (br s, 1H, $NCH_2$), 6.14 (t, $J_{H,H}$ = 5.1 Hz, 1H, NH), 4.60 (br s, 1H, $NCH_2$), 4.53 (s, 1H, NBD), 3.88 (br s, 1H, $CH_2NH$), 3.72 (br s, 1H, $CH_2NH$), 3.62 (s, 1H, CH, NBD), 3.57 (s, 1H, CH, NBD), 3.23 (s, 1H, CH, NBD), 2.82 (s, 1H, CH, NBD), 2.1 (s, 1H, CH, NBD), 1.41 (s, 9H, $^t$Bu), 0.98 (m, 2H, NBD). $^{13}C\{^1H\}$ NMR (150.8 MHz, $CDCl_3$, 243.2 K): $\delta$ 185.4 (d, $J_{C,Rh}$ = 56.1 Hz), 156.6 (C═O), 142.1 ($C_5$), 128.7 ($C_4$), 128.3 ($C_2$), 127.4 ($C_3$), 124.8 ($CH_{im}$), 119.7 ($CH_{im}$), 79.1 (Cq, $^t$Bu), 77.3 ($C_1$), 73.5 (CH, NBD), 64.3 (CH, NBD), 61.9 ($C^7H_2$, $J_{C,Rh}$ = 5.1 Hz, NBD), 51.2 ($NCH_2$), 49.3 (CH, NBD), 48.7 (CH, NBD), 45.1 (CH, NBD), 44.7 (CH, NBD), 40.8 ($CH_2NH$), 28.8 ($CH_3$, $^t$Bu). IR ($CH_2Cl_2$, $cm^{-1}$): 1702 (vs, $\nu_{CO}$). IR (KBr, $cm^{-1}$): 3319 (s, $\nu_{NH}$), 3141, 3089, 3058, 3032, 2975, 2930, 1707 (vs, $\nu_{CO}$), 1492, 1445, 1250, 1170. ESI-MS (MeOH, *m/z*): 648 (100) $[M - Cl]^+$; 682 $[M - H]^-$. Anal. Calcd (%) for $C_{36}H_{39}ClN_3O_2Rh$: C, 63.21; H, 5.75; N, 6.14. Found: C, 63.51; H, 5.98; N, 6.04. Mp = 108 °C.

**Synthesis of [Rh(NBD)I{1-(2-NHBoc-ethyl)-3-methylimidazolin-2-ylidene}], 4a, by Method B (iii).** $[Rh(NBD)Cl]_2$ (0.050 g, 0.11 mmol) and KO$^t$Bu (0.024 g, 0.22 mmol) were reacted in THF (10 mL) for 3 h. Successively the imidazolium salt **1a** (0.076 g, 0.212 mmol) was added, and after stirring for a further 3 h the solid was removed by filtration and the resulting orange solution was evaporated to dryness. After washing with $Et_2O$ 0.049 g (41%) of **4a** was obtained, and suitable crystals of **4a** for X-ray diffraction have been obtained by slow evaporation from a mixture of $CH_2Cl_2$ and petroleum ether.

**Synthesis of 4a by Ion Exchange.** Alternatively to a solution of **3a** (0.050 mg, 0.11 mmol) in degassed methanol (2 mL) was added an excess of NaI (0.030 g, 0.2 mmol). After stirring for 20 h the suspension was filtered, and after removal of the volatiles *in vacuo* the product was used without further workup. $^1$H NMR (399.9 MHz, $CDCl_3$): $\delta$ 6.78 (s, 2H, $CH_{im}$), 5.25 (br s, 1H, NH), 5.09 (m, 1H, CH, NBD), 4.98 (m, 1H, CH, NBD), 4.64 (m, 1H, $NCH_2$), 4.26 (m, 1H, $NCH_2$), 3.98 (s, 3H,

$CH_3$), 3.89 (m, 1H, $CH_2NH$), 3.82 (m, 2H, CH, NBD), 3.72 (m, 1H, $CH_2NH$), 3.63 (m, 2H, CH, NBD), 1.42 (s, 9H, $^t$Bu), 1.26 (m, 2H, $CH_2$, NBD). $^{13}C\{^1H\}$ NMR: $\delta$ 183.7 (d, $J_{C,Rh}$ = 56.2 Hz), 122.0 ($CH_{im}$), 121.9 ($CH_{im}$), 78.9 (Cq, $^t$Bu), 76.8 (CH, NBD), 76.4 (CH, NBD), 64.9 ($^7CH_2$, NBD), 49.2 ($NCH_2$), 37.7 ($CH_3$), 40.3 ($CH_2NH$), 51.2 (CH, NBD), 50.6 (CH, NBD), 28.0 ($^t$Bu). IR (THF, $cm^{-1}$): $\nu$(C═O): 1715. IR (KBr, $cm^{-1}$): 3354 (s, $\nu_{NH}$), 3165, 3094, 3052 (m, $CH_{im}$), 2975, 2924 (br vs, CH), 1700 (vs, $\nu_{CO}$). ESI-MS(+) (MeOH, $m/z$): 420 (100) $[M - I]^+$; 127 (100) $[I^-]$. Anal. Calcd (%) for $C_{18}H_{27}IN_3O_2Rh$: C, 39.51; H, 4.97; N, 7.68. Found: C, 40.00; H, 5.14; N, 7.61. Mp = 148 °C (dec).

**X-ray Crystal Structure Determination for 1c, 3a, 4a, and 3c.** Crystal data were collected at room temperature on a Bruker APEX II diffractometer equipped with a CCD detector operating at 50 kV and 30 mA, using graphite-monochromated Mo K$\alpha$ radiation ($\lambda$ = 0.71073 Å). An empirical absorption correction was applied on both structures by using SADABS.[35] They were solved by direct methods and refined by full-matrix least-squares based on all data using $F^2$ with SHELXL97.[36] All non-hydrogen atoms were refined anisotropically, with the exception of the hydrogen atoms, which were set geometrically and given fixed isotropic thermal parameters. There is a positional disorder in the structure of $C_{18}H_{27}IN_3O_2Rh$ (**4a**), more specifically in the *tert*-butyl group, so the involved carbon atoms were split in two positions, and anisotropic displacement parameter restraints were applied. Crystal data are collected in Table 2.

**Variable-Temperature NMR.** NMR spectra were recorded using spectrometers operating at fields of 9.6 and 14.4 T (400 and 600 MHz for $^1$H). The NMR tubes containing the compounds were prepared under an argon atmosphere using a vacuum line. Low-temperature $^1$H spectra were acquired without spinning using a 5 mm dual direct probe with a 6000 Hz (at 400 MHz) or 9000 Hz (at 600 MHz) sweep width, 40° tip angle pulse width, 3 s acquisition time, and 1 s delay time. A shifted sine bell weighting function equal to the acquisition time (i.e., 3 s) was applied before the Fourier transformation. Usually 32 to 64 scans were collected. When operating the NMR apparatus at low temperature, a flow of dry nitrogen was first passed through a precooling unit adjusted to −50 °C. Then the gas entered into an inox steel heat-exchanger immersed in liquid nitrogen and connected to the NMR probe head by a vacuum-insulated transfer line. Gas flows of 10 to 20 L $min^{-1}$ were required to descend to the desired temperature. Temperature calibrations were performed before the experiments, using a digital thermometer and a Cu/Ni thermocouple placed in an NMR tube filled with isopentane for the low-temperature range and with tetrachloroethane for the high-temperature range. The conditions were kept as identical as possible with all subsequent work. In particular, the sample was not spun and the gas flow was the same as that used during the acquisition of the spectra. The uncertainty in temperature measurements can be estimated from the calibration curve as ±2 °C.

Line shape simulations were performed using a PC version of the QCPE DNMR6 program.[37] Electronic superimposition of the original spectrum and of the simulated one enabled the determination of the most reliable rate constant. The rate constants, thus obtained at various temperatures, afforded the free energy of activation $\Delta G^{\ddagger}$ by applying the Eyring equation.[38] $\Delta H^{\ddagger}$ and $\Delta S^{\ddagger}$ were evaluated by linear regression of the $\Delta G^{\ddagger}$ value vs the temperature. Except for **3c**, in all cases investigated, the activation energy $\Delta G^{\ddagger}$ was found to be virtually invariant in the given temperature range, thus implying a very small or negligible activation entropy $\Delta S^{\ddagger}$.[19,39]

**DFT Calculations.** Conformational searches were performed by Molecular Mechanics (MMFF force field as implemented in Titan 1.0.5, Wavefunction Inc.). Final geometry optimizations were carried out at the B3LYP/LanL2DZ level[40] by means of the Gaussian 09 series of programs[41] (see the Supporting Information). The standard Berny algorithm in redundant internal coordinates and default criteria of convergence were employed in all the calculations. Harmonic vibrational frequencies were calculated for all the stationary points. For each optimized ground state the frequency analysis showed the absence of imaginary frequencies, whereas each transition state showed a single imaginary frequency. Visual inspection of the corresponding normal mode was used to confirm that the correct transition state had been found. All the reported energy values represent total electronic energies. In general, these give the best fit with experimental DNMR data.[42] Therefore, the computed numbers have not been corrected for zero-point energy contributions or other thermodynamic parameters. This avoids artifacts that might result from the ambiguous choice of the adequate reference temperature, from the empirical scaling,[43] and from the treatment of low-frequency vibration as harmonic oscillators.[44]

**Catalysis.** *General Procedure for the Hydrosilylation of 1-Alkynes with $HSiMe_2Ph$.* A J. Young valve NMR tube was charged under argon with the catalyst precursor (**3a**−**c**) ($7.7 \times 10^{-4}$ mmol), $CDCl_3$ (0.6 mL), the corresponding alkyne (PhC≡CH, TolC≡CH, $^n$BuC≡CH, $Et_3SiC$≡CH, or $(CPh_2OH)C$≡CH) (0.077 mmol), and a slight excess of $HSiMe_2Ph$ (0.085 mmol). The solution was kept at $T$ = 25 °C and monitored by $^1$H NMR spectroscopy. The new products were characterized by $^1$H NMR and by comparison with similar compounds reported in the literature.[25]

*(E)-2-(Dimethyl(phenyl)silyl)-1-tolylethene.* $^1$H NMR (300.1 MHz, $CDCl_3$): $\delta$ 7.60−7.16 (m, 9H), 6.96 (d, 1H, $J_{H,H}$ = 19.2 Hz), 6.45 (d, 1H, $J_{H,H}$ = 19.2 Hz,), 2.36 (s, 3H), 0.49 (s, 6H) ppm.

*1-(Dimethyl(phenyl)silyl)-1-tolylethene.* $^1$H NMR (300,1 MHz, $CDCl_3$): $\delta$ 7.6−7.3 (m, 4H), 5.93 (d, 1H, $J_{H,H}$ = 2.9 Hz), 5.66 (d, 1H, $J_{H,H}$ = 2.9 Hz), 2.35 (s, 3H), 0.30 (s, 6H) ppm.

*(E)-2-(dimethylphenylsilyl)-1-($CPh_2OH$)ethene.* $^1$H NMR (300,1 MHz, $CDCl_3$): $\delta$ 7.77−7.24 (m, 15H), 6.74 (d, 1H, $J_{H,H}$ = 18.8 Hz), 6.16 (d, 1H, $J_{H,H}$ = 18.8), 0.35 (s, 6H).

*1-(Dimethylphenylsilyl)-1-($CPh_2OH$)ethene.* $^1$H NMR (300,1 MHz, $CDCl_3$): $\delta$ 7.77−7.24 (m, 15H), 5.72 (d, 1H, $J_{H,H}$ = 1.8), 5.28 (d, 1H, $J_{H,H}$ = 1.8), 0.39 (s, 6H).

*General Procedure for the Addition of Arylaldehydes with Phenylboronic Acid.* Phenylboronic acid (0.600 g, 4.9 mmol), KO$^t$Bu (2.45 mmol), the substituted aldehyde (4-chlorobenzaldehyde, 4-methoxybenzaldehyde, 3,4,5-trimethoxybenzaldehyde, 4-*tert*-butylbenzaldehyde, 4-cianobenzaldehyde, 4-acetylbenzaldehyde) (2.45 mmol), the rhodium catalyst **3a** or **3b** (1% mol), and dimethoxyethane (7.5 mL) were introduced in a Schlenck tube, and then degassed $H_2O$ (2.5 mL) was added. The resulting mixture was heated for 1−8 h at 80 °C, cooled to ambient temperature, and extracted with ethyl acetate (20 mL). After drying over $Na_2SO_4$ the organic phase was evaporated, and the residue was purified by flash chromatography. The isolated yield was checked by $^1$H NMR spectroscopy. The reaction products were identified by NMR comparison with literature reported data.[28]

## ■ ASSOCIATED CONTENT

**Supporting Information.** Computational details; structural data for **1c**, **3a**, **4a**, **3c**; $^1$H, $^{13}$C, and HSQC NMR spectra for **3c**; VT NMR for **3a**, **4a**, **3c**; details and full characterization data for the catalysis. X-ray data in the form of CIF files. This material is available free of charge via the Internet at http://pubs.acs.org.

## ■ AUTHOR INFORMATION

### Corresponding Author

*E-mail: maria.cassani@unibo.it (M.C.C.), rita.mazzoni@unibo.it (R.M.). Fax: +39 0512093694. Phone: +39 051 2093700.

## ■ ACKNOWLEDGMENT

The authors thank the University of Bologna and the Ministero dell'Università e della Ricerca (MUR) (project: "New strategies for

the control of reactions: interactions of molecular fragments with metallic sites in unconventional species", PRIN 2007) for financial support.

## REFERENCES


(1) For reviews on N-heterocyclic carbenes see: (a) Mercs, L.; Albrecht, M. *Chem. Soc. Rev.* **2010**, *39*, 1903. (b) Diez-Gonzalez, S.; Marion, N.; Nolan, S. P. *Chem. Rev.* **2009**, *109*, 3612. (c) Jacobsen, H.; Correa, A.; Poater, A.; Costabile, C.; Cavallo, L. *Coord. Chem. Rev.* **2009**, *253*, 687. (d) Hahn, F. E., Ed. of themed issue: N-Heterocyclic Carbenes. *Dalton Trans.* **2009**, *35*, 6873. (e) Hahn, F. E.; Jahnke, M. C. *Angew. Chem., Int. Ed.* **2008**, *47*, 3128. (f) Crabtree, R. H. *Coord. Chem. Rev.* **2007**, *251*, 595 ff, a volume completely dedicated to recent developments in the organometallic chemistry of N-heterocyclic carbenes. (g) Crudden, C. M.; Allen, D. P. *Coord. Chem. Rev.* **2004**, *248*, 2247. (h) Herrmann, W. A. *Angew. Chem., Int. Ed.* **2002**, *41*, 1290. (i) Bourissou, D.; Guerret, O.; Gabbai, F. P.; Bertrand, G. *Chem. Rev.* **2000**, *100*, 39.

(2) (a) Bierenstiel, M.; Cross, E. D. *Coord. Chem. Rev.* **2011**, *255*, 574. (b) Corberan, R.; Mas-Marzà, E.; Peris, E. *Eur. J. Inorg, Chem.* **2009**, 1700. (c) Normand, A. T.; Cavell, K. J. *Eur. J. Inorg. Chem.* **2008**, 2781. (d) Kühl, O. *Chem. Soc. Rev.* **2007**, *36*, 592. (e) Pugh, D.; Danopoulos, A. A. *Coord. Chem. Rev.* **2007**, *251*, 610. (f) Liddle, S. T.; Edworthy, I. S.; Arnold, P. L. *Chem. Soc. Rev.* **2007**, *36*, 1732.

(3) (a) Morris, R. H. *Chem. Soc. Rev.* **2009**, *38*, 2282. (b) Gaillard, S.; Renaud, J. L. *ChemSusChem* **2008**, *1*, 505. (c) Mikhailine, A.; Lough, A. J.; Morris, R. H. *J. Am. Chem. Soc.* **2009**, *131*, 1394. (d) Jiménez, M. V.; Pérez-Torrente, J. J.; Bartolomè, M. I.; Gierz, V.; Lahoz, F. J.; Oro, L. A. *Organometallics* **2008**, *27*, 224. (e) Flahaut, A.; Roland, S.; Mangeney, P. *Tetrahedron: Asymmetry* **2007**, *18*, 229. (f) Edworthy, I. S.; Rodden, M.; Mungur, S. A.; Davis, K. M.; Blake, A. J.; Wilson, C.; Schrőder, M.; Arnold, P. L. *J. Organomet. Chem.* **2005**, *690*, 5710. (g) Douthwaite, R. E.; Houghton, J.; Kariuki, B. M. *Chem. Commun.* **2004**, 698. (h) Arnold, P. L.; Mungur, S. A.; Blake, A. J.; Wilson, C. *Angew. Chem., Int. Ed.* **2003**, *42*, 5981. (i) Herrmann, W. A.; Köcher, C.; Gooßen, L. J.; Artus, G. R. J. *Chem.—Eur. J.* **1996**, *2*, 1627.

(4) (a) Langkopf, E.; Schinzer, D. *Chem. Rev.* **1995**, *95*, 1375. (b) Roy, A. K. *Adv. Organomet. Chem.* **2008**, *55*, 1, and references therein.

(5) (a) Yigit, M.; Ozdemir, I.; Cetinkaya, E.; Cetinkaia, B. *Transition Met. Chem* **2007**, *32*, 536. (b) Karaaslan, R.; Yigit, M.; Ozdemir, I.; Cetinkaya, E.; Cetinkaya, B. *J. Heterocycl. Chem.* **2007**, *44*, 69, and reference therein. (c) Gois, P. M. P.; Trindade, A. F.; Veiros, L. F.; Andrè, V.; Duarte, M. T.; Afonso, C. A. M.; Caddick, S.; Cloke, F. G. N. *Angew. Chem., Int. Ed.* **2007**, *46*, 5750. (d) Imlinger, N.; Mayr, M.; Wang, D.; Wurst, K.; Buchmeiser, M. R. *Adv. Synth. Catal.* **2004**, *346*, 1836. (e) Furstner, A.; Krause, H. *Adv. Synth. Catal.* **2001**, *343*, 343.

(6) Ozdemir, I.; Gurbuz, N.; Gok, Y.; Cetinkaya, B.; Cetinkaya, E. *Transition Met. Chem.* **2005**, *30*, 367.

(7) Busetto, L.; Cassani, M. C.; Femoni, C.; Macchioni, A.; Mazzoni, R.; Zuccaccia, D. *J. Organomet. Chem.* **2008**, *693*, 2579.

(8) Ballarin, B.; Busetto, L.; Cassani, M. C.; Femoni, C. *Inorg. Chim. Acta* **2010**, *363*, 2055.

(9) Ballarin, B.; Cassani, M. C.; Tonelli, D.; Boanini, E.; Albonetti, S.; Blosi, M.; Gazzano, M. *J. Phys. Chem. C* **2010**, *114*, 9693.

(10) Ballarin, B.; Cassani, M. C.; Gazzano, M.; Solinas, G. *Electrochim. Acta* **2010**, *56*, 676.

(11) Park, K. H.; Kim, S. Y.; Son, S. U.; Chung, Y. K. *Eur. J. Org. Chem.* **2003**, 4341.

(12) Lough, W. W. N. O, A. J.; Morris, R. H. *Organometallics* **2009**, *28*, 6755, and references therein.

(13) Navarro, M.; Cisneros-Fajardo, E. J.; Lehmann, T.; Sanchez-Delgado, R. A.; Atencio, R.; Silva, P.; Lira, R.; Urbina, J. A. *Inorg. Chem.* **2001**, *40*, 6879.

(14) (a) Casarini, D.; Femoni, C.; Grilli, S.; Lunazzi, L.; Mazzanti, A. *J. Org. Chem.* **2001**, *66*, 488. (b) Gust, D.; Mislow, K. *J. Am. Chem. Soc.* **1973**, *95*, 1535. (c) Focante, F.; Leardini, R.; Mazzanti, A.; Mercandelli, P.; Nanni, D. *Organometallics* **2006**, *25*, 2166.

(15) (a) Wang, H. M. J.; Lin, I. J. B. *Organometallics* **1998**, *17*, 972. (b) Chianese, A. R.; Li, X.; Janzen, M. C.; Faller, J. W.; Crabtree, R. H. *Organometallics* **2003**, *22*, 1663. (c) Lin, I. J. B.; Vasam, C. S. *Coord. Chem. Rev.* **2007**, *251*, 642.

(16) Herrmann, W. A.; Gooβen, L. J.; Spiegler, M. *J. Organomet. Chem.* **1997**, *547*, 357.

(17) (a) Hirai, K.; Nutton, A.; Maitlis, P. *J. Mol. Catal.* **1981**, *10*, 203. (b) Lei, A.; He, M.; Zhang, X. *J. Am. Chem. Soc.* **2002**, *124*, 8198, and references therein.

(18) Jong, H.; Patrick, B. O.; Fryzuk, M. D. *Can. J. Chem.* **2008**, *86*, 803.

(19) For a review see: Casarini, D.; Lunazzi, L.; Mazzanti, A. *Eur. J. Org. Chem.* **2010**, 2035.

(20) (a) Enders, D.; Gielen, H.; Runsink, J.; Breuer, K.; Brode, S.; Boehn, K. *Eur. J. Inorg. Chem.* **1998**, 913. (b) Enders, D.; Gielen, H. *J. Organomet. Chem.* **2001**, *617*, 70.

(21) (a) Korenaga, T.; Aikawa, K.; Terada, M.; Kawauchi, S.; Mikami, K. *Adv. Synth. Catal.* **2001**, *343*, 284. (b) Mikami, K.; Aikawa, K.; Yusa, Y.; Jodry, J. J.; Yamanaka, M. *Synlett* **2002**, *10*, 1561. (c) Fjellander, E.; Szabó, Z.; Moberg, C. *J. Org. Chem.* **2009**, *74*, 9120.

(22) (a) Oki, M. *Pure Appl. Chem.* **1989**, *61*, 699. (b) Oki, M.; Shimizu, A.; Kihara, H.; Nakamura, N. *Chem. Lett.* **1980**, *9*, 607.

(23) (a) Ojima, I.; Vu, A. T.; Boonafux, D. *Science of Synthesis Vol. 1*; Lautens, M., Ed.; Georg Thieme Verlag: Stuttgart, 2001; section 1.5. (b) Bleeke, J. R.; Donaldson, A. J. *Organometallics* **1988**, *7*, 1588.

(24) Since the detrimental effect on the reaction rate of the steric hindrance on the NHC ligand was already demonstrated employing **3a**−**c** with PhC≡CH, TolC≡CH, and $^n$BuC≡CH, the effect of the steric encumbrance of the alkynes $Et_3SiC{\equiv}CH$ and $(CPh_2OH)C{\equiv}CH$ has been tested only with the best catalyst **3a**.

(25) The vinylsilane, alkene, and allyl derivatives were unambiguously characterized by $^1$H NMR spectroscopy by comparison with literature spectra, when available, or by comparison with spectra of similar compounds. Derivatives from PhC≡CH: (a) Nakamura, S.; Uchiyama, M.; Ohwada, T. *J. Am. Chem. Soc.* **2004**, *126*, 11146. (b) Nishihara, Y.; Saito, D.; Tanemura, K.; Noyori, S.; Takagi, K. *Org. Lett.* **2009**, *11*, 3546. Derivatives from TolC≡CH: (c) Katayama, H.; Taniguchi, K.; Kobayashi, M.; Sagawa, T. *J. Organomet. Chem.* **2002**, *645*, 192. See also the Experimental Section. Derivatives from $^n$BuC≡CH: (d) Jun, C. H.; Crabtree, R. H. *J. Organomet. Chem.* **1993**, *447*, 177. (e) Schwieger, S.; Herzog, R.; Wagner, C.; Steinborn, D. *J. Organomet. Chem.* **2009**, *694*, 3548 Derivatives from $Et_3SiC{\equiv}CH$: see ref 3d. Derivatives from $(CPh_2OH)C{\equiv}CH$: see the Experimental Section and the Supporting Information.

(26) (a) Poyatos, M.; Mas-Marzà, E.; Mata, J. A.; Sanau, M.; Peris, E. *Eur. J. Inorg, Chem.* **2003**, 1215. (b) Ojima, I.; Clos, N.; Donovan, R. J.; Ingallina, P. *Organometallics* **1990**, *9*, 3127.

(27) de Bo, G.; Berthoz-Gelloz, G.; Tinant, B.; Markò, I. E. *Organometallics* **2006**, *25*, 1881.

(28) Since the detrimental effect on the reaction rate of the steric hindrance on the NHC ligand was already demonstrated employing **3a**, **b**, the addition of arylaldehydes with phenylboronic acid has not been tested with the more encumbered **3c**.

(29) The secondary alcohol derivatives were unambiguously characterized by comparison with literature NMR spectra. (a) Xing, C.-H.; Hu, Q.-S. *Tetrahedron Lett.* **2010**, *51*, 924. (b) Kuriyama, M.; Ishiyama, N.; Shimazawa, R.; Onomura, O. *Tetrahedron* **2010**, *66*, 6814. (c) Krasovskiy, A.; Straub, B. F.; Knochel, P. *Angew. Chem., Int. Ed.* **2005**, *45*, 159. (d) Umeda, R.; Studer, A. *Org. Lett.* **2008**, *10*, 993. See also the Supporting Information.

(30) (a) Yoshida, K.; Hayashi, T. In *Boronic Acids*; Hall, D. G., Ed.; Wiley-VCH: Weinheim, 2005; Chapter 4, pp 172−203. (b) Sakai, M.; Ueda, M.; Miyaura, N. *Angew. Chem., Int. Ed.* **1998**, *37*, 3279.

(31) Sigler, G. F.; Riaz, R. Patent WO2000078763, 2000.

(32) Bridger, G. J.; Skerlj, R. T.; Kaller, A.; Harwig, C.; Bogucki, D.; Wilson, T.; Crawford, J.; McEachern, E. J.; Atsma, B.; Nan, S.; Zhou, Y.; Schols, D.; Smith, C. D.; Di Fluri, R. M. Patent WO2003055876, 2003. The yield for $BocNHCH_2CH_2Im$ has been improved up to 77%, eluting

the chromatography column with $CH_2Cl_2$/MeOH/$NH_4OH$, 100:5−100:5:1.

(33) Perrin, D. D.; Armarego, W. L. F.; Perrin, D. R. *Purification of Laboratory Chemicals*, 2nd ed.; Pergamon Press: New York, 1980.

(34) Neumann, W. P.; Uzick, W.; Zarkadis, Antonios, K. *J. Am. Chem. Soc.* **1986**, *108*, 3762.

(35) Sheldrick, G. M. *SADABS*; University of Göttingen, Germany, 1996.

(36) Sheldrick, G. M. *SHELXL97*; University of Gottingen, Germany.

(37) Brown, J. H.; Bushweller, C. H. *QCPE* **1983**, *3*, 103. A copy of the program is available on request from the authors (A.M. and M.M.)

(38) Eyring, H. *Chem. Rev.* **1935**, *17*, 65.

(39) Lunazzi, L.; Mancinelli, M.; Mazzanti, A. *J. Org. Chem.* **2007**, *72*, 5391.

(40) For B3LYP functional: (a) Becke, A. D. *J. Chem. Phys.* **1993**, *98*, 5648. (b) Lee, C.; Yang, W.; Parr, R. G. *Phys. Rev. B* **1988**, *37*, 785. (c) Stephens, P. J.; Devlin, F. J.; Chabalowski, C. F.; Frisch, M. J. *J. Phys. Chem.* **1994**, *98*, 11623. For the LanL2DZ basis set: (d) Hay, P. J.; Wadt, W. R. *J. Chem. Phys.* **1985**, *82*, 299.

(41) Frisch, M. J.; Trucks, G. W.; Schlegel, H. B.; Scuseria, G. E.; Robb, M. A.; Cheeseman, J. R.; Scalmani, G.; Barone, V.; Mennucci, B.; Petersson, G. A.; Nakatsuji, H.; Caricato, M.; Li, X.; Hratchian, H. P.; Izmaylov, A. F.; Bloino, J.; Zheng, G.; Sonnenberg, J. L.; Hada, M.; Ehara, M.; Toyota, K.; Fukuda, R.; Hasegawa, J.; Ishida, M.; Nakajima, T.; Honda, Y.; Kitao, O.; Nakai, H.; Vreven, T.; Montgomery, Jr., J. A.; Peralta, J. E.; Ogliaro, F.; Bearpark, M.; Heyd, J. J.; Brothers, E.; Kudin, K. N.; Staroverov, V. N.; Kobayashi, R.; Normand, J.; Raghavachari, K.; Rendell, A.; Burant, J. C.; Iyengar, S. S.; Tomasi, J.; Cossi, M.; Rega, N.; Millam, N. J.; Klene, M.; Knox, J. E.; Cross, J. B.; Bakken, V.; Adamo, C.; Jaramillo, J.; Gomperts, R.; Stratmann, R. E.; Yazyev, O.; Austin, A. J.; Cammi, R.; Pomelli, C.; Ochterski, J. W.; Martin, R. L.; Morokuma, K.; Zakrzewski, V. G.; Voth, G. A.; Salvador, P.; Dannenberg, J. J.; Dapprich, S.; Daniels, A. D.; Farkas, Ö.; Foresman, J. B.; Ortiz, J. V.; Cioslowski, J.; Fox, D. J. *Gaussian 09* rev A.02; Gaussian, Inc.: Wallingford, CT, 2009.

(42) Ayala, P. Y.; Schlegel, H. B. *J. Chem. Phys.* **1998**, *108*, 2314.

(43) Tormena, C. F.; Rittner, R.; Abraham, R. J.; Basso, E. A.; Fiorin, B. C. *J. Phys. Org. Chem.* **2004**, *17*, 42.

(44) (a) Wong, M. W. *Chem. Phys. Lett.* **1996**, *256*, 391. (b) Wheeler, S. E.; McNeil, A. J.; Müller, P.; Swager, T. M.; Houk, K. N. *J. Am. Chem. Soc.* **2010**, *132*, 3304.